Modeling of the cardiac sympathetic nervous system and the contribution of epicardium-derived cells

Ge, Y.

PART I

CARDIAC SYMPATHETIC INNERVATION AND EPDCS

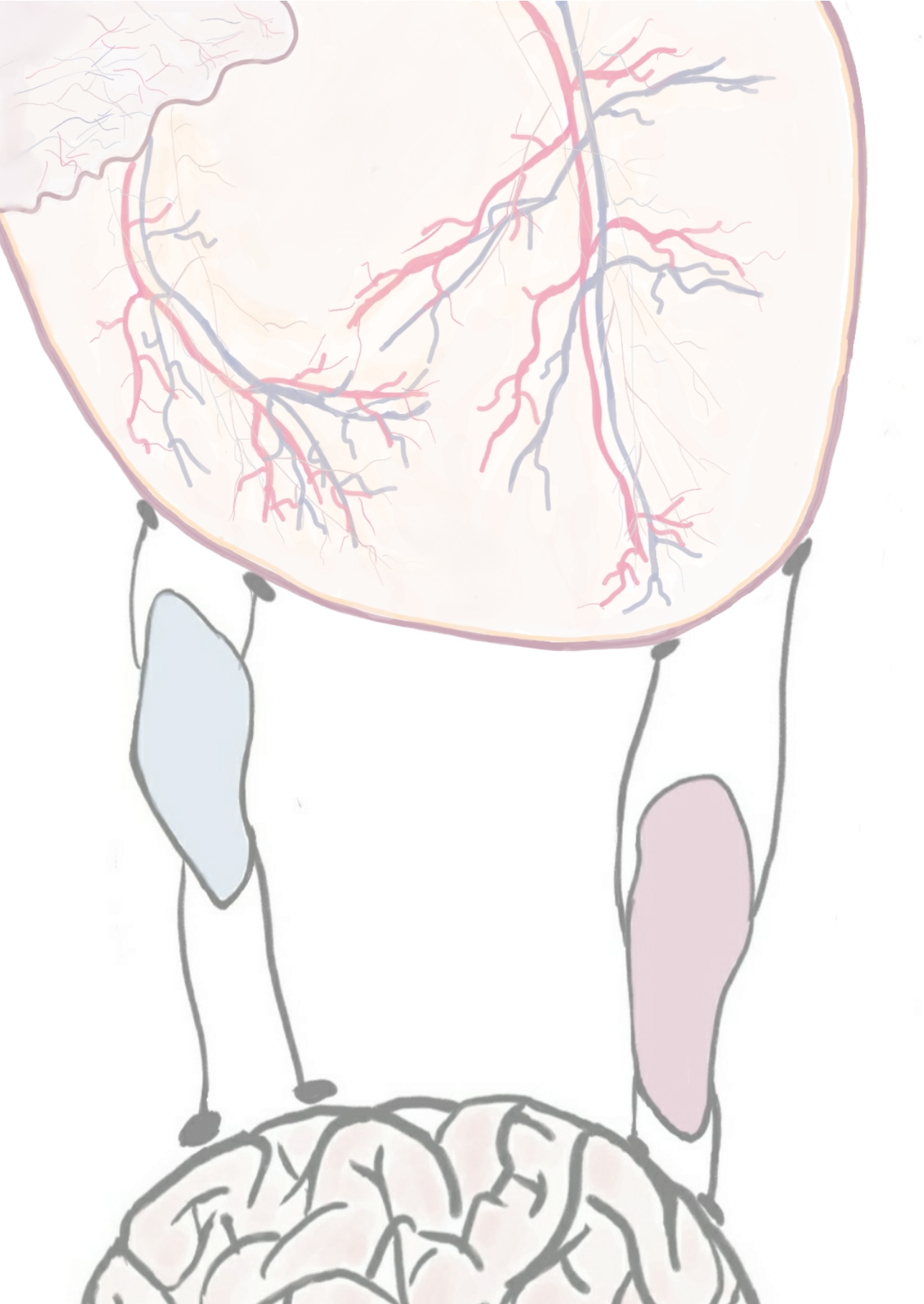

2

HUMAN EPICARDIUM-DERIVED CELLS REINFORCE CARDIAC SYMPATHETIC INNERVATION

Yang Ge[1,2], Anke M. Smits[3], J. Conny van Munsteren[1], Adriana C. Gittenberger-de Groot[2], Robert E. Poelmann[2], Thomas J. van Brakel[2], Martin J. Schalij[2], Marie-José T.H. Goumans[3], Marco C. DeRuiter[1], Monique R.M. Jongbloed[1,2]

a. Department of Anatomy & Embryology, Leiden University Medical Center, Einthovenweg 20, 2333 ZC Leiden, The Netherlands;

b. Department of Cardiology and Thoracic Surgery, Leiden University Medical Center, Albinusdreef 2, 2333 ZC Leiden, The Netherlands;

c. Department of Cell and Chemical Biology, Leiden University Medical Center, Einthovenweg 20, 2333 ZC Leiden, The Netherlands;

J Mol Cell Cardiol 2020 Jun;143:26-37. doi: 10.1016/j.yjmcc.2020.04.006

ABSTRACT

Rationale: After cardiac damage, excessive neurite outgrowth (sympathetic hyperinnervation) can occur, which is related to ventricular arrhythmias/sudden cardiac death. Post-damage reactivation of epicardium causes epicardium-derived cells (EPDCs) to acquire a mesenchymal character, contributing to cardiac regeneration. Whether EPDCs also contribute to cardiac re/hyperinnervation, is unknown.

Aim: To investigate whether mesenchymal EPDCs influence cardiac sympathetic innervation.

Methods and results: Sympathetic ganglia were co-cultured with mesenchymal EPDCs and/or myocardium, and neurite outgrowth and sprouting density were assessed. Results showed a significant increase in neurite density and directional (i.e. towards myocardium) outgrowth when ganglia were co-cultured with a combination of EPDCs and myocardium, as compared to cultures with EPDCs or myocardium alone. In absence of myocardium, this outgrowth was not directional. Neurite differentiation of PC12 cells in conditioned medium confirmed these results via a paracrine effect, in accordance with expression of neurotrophic factors in myocardial explants co-cultured with EPDCs. Of interest, EPDCs increased the expression of nerve growth factor (NGF) in cultured, but not in fresh myocardium, possibly due to an "ischemic state" of cultured myocardium, supported by TUNEL and Hif1α expression. Cardiac tissues after myocardial infarction showed robust NGF expression in the infarcted, but not remote area.

Conclusion: Neurite outgrowth and density increases significantly in the presence of EPDCs by a paracrine effect, indicating a new role for EPDCs in the occurrence of sympathetic re/hyperinnervation after cardiac damage.

Keywords

Epicardium-derived cells (EPDCs); Nerve growth factor (NGF); Neurite outgrowth; Semaphorin 3A (SEMA3A); Sympathetic hyperinnervation.

INTRODUCTION

Cardiac function is influenced by the cardiac autonomic nervous system tone. Cardiac sympathetic stimulation increases heart rate, contraction force and atrioventricular conduction velocity, whereas parasympathetic stimulation largely results in opposite effects. Balanced cardiac sympathetic and parasympathetic activity is critical for maintaining normal cardiac function. Excessive sympathetic activation can be pro-arrhythmogenic, whereas parasympathetic activation is considered to be cardioprotective [1,2]. An accumulating amount of reports indicate a relation between ventricular arrhythmias, sudden cardiac death and activity of the sympathetic autonomic nervous system [3,4]. Although sudden cardiac death after myocardial infarction (MI) is in general attributed to heterogeneous conduction in the infarct border zone [5], autonomic hyperinnervation after MI is also related to sudden cardiac death in numerous reports [6,7]. In addition, sympathetic hyperinnervation has been described in other states of cardiac damage/overload, such as hypertension, RV overload and pulmonary hypertension [8,9].

The definition of post-MI sympathetic hyperinnervation is most often linked to an increase of sympathetic nerve sprouting which can be observed between 3h to several months after the cardiac event [10]. The increased sympathetic nerve density is considered to result from sprouting from cardiac sympathetic ganglia, clusters of neuron cell bodies located bilaterally to the spinal cord at cervical and upper thoracic levels [11].

During development, ventricular innervation develops in close relationship with ventricular vascularization and axons use the developing coronary veins as guides. Neurotrophic factors secreted by coronary veins/epicardium-derived smooth muscle cells guide this process [12,13].

The epicardium is a monolayer of tissue covering the heart. Although it is predominantly quiescent in the healthy adult heart, in the fetal phase it is a multipotent population with various functions. Cells derived from the epicardium, so called epicardium-derived cells (EPDCs), function as a powerful population of cardiac progenitor cells [14–16]. EPDCs expressing e.g.Tbx18, Tcf21 and WT1 can undergo a process known as epithelial-to-mesenchymal transition (EMT) [17,18]. These post-EMT EPDCs acquire mesenchymal cell characteristics and the ability to migrate and populate the subepicardial space by differentiating into different cell types [16]. Of interest, the fetal epicardium also transiently expresses the β2-adrenergic receptor (β2-AR), and was shown to be essential for the early autonomic response [19].

In the adult, epicardium can get reactivated after cardiac damage such as MI. After reactivation, EPDCs regain an embryonic phenotype with an enrichment of EPDCs in the

infarcted area [15,20,21]. Exogenous administrated adult-derived mesenchymal EPDCs have also been shown to migrate to the infarcted area where they contribute to neovascularization and amelioration of left ventricular function [22]. Whether EPDCs also contribute to cardiac re-innervation as is shown after MI, is currently not known.

The current study is aimed at exploring the effect of adult-derived mesenchymal EPDCs on cardiac sympathetic innervation and demonstrates that these potent cells promote sympathetic nerve sprouting towards "damaged" cultured adult myocardium in vitro.

MATERIALS AND METHODS

A detailed overview of methodology for all sections described below, is provided in the Supplemental Materials.

Experimental animals

C57BL/6 J (Jackson Laboratory) adult mice (n = 42) and mice embryos of embryonic day (E) 18.5 (n = 81) were used. All animal experiments were carried out according to the Guide for the Care and Use of Laboratory Animals published by NIH and approved by the Animal Ethics Committee of the Leiden University (License number AVD1160020185325), Leiden, The Netherlands).

MI induction

8-week male C57BL/6 J mice (n = 4) were anesthetized with isoflurane 5% for induction and 1.5–2% for maintenance. MI was induced by permanent ligation of left anterior descending coronary artery for 7 days [22].

Isolation and culture of human EPDCs

EPDCs were isolated from adult human cardiac tissue and EMT was induced as previously described [23,24]. Briefly, the epicardium was carefully peeled off and cells were dissociated, to exclude contamination with other cells. Isolated EPDCs of epithelial state have a typical cuboidal morphology, therefore EPDCs can readily be distinguished from other cell types. Only cultures that displayed a clear epithelial morphology were used for further experiments to ensure their derivation from the epicardium. Mesenchymal EPDCs were obtained after several days of TGFβ stimulation and were cultured for several passages in an mesenchymal state. Mesenchymal post-EMT EPDC are characterized by their morphology and gene expression pattern (Supplemental fig. S1). Human mesenchymal EPDCs of passage 6 to 9 were prepared into aggregates and cultured for 4 days until ready for further co-culture. All experiments were

performed according to the guidelines of the Leiden University Medical Centre (Leiden, The Netherlands) and according to the Dutch regulations on the use of human tissues. The study was conducted according to the principles of the Declaration of Helsinki (64th WMA General Assembly, Fortaleza, Brazil, October 2013) and national and institutional guidelines, regulations and acts.

Dissection and culture of adult murine myocardium

Pregnant mice were euthanized in a CO2 chamber. Left ventricular myocardium was isolated from mother mice and processed into pieces of similar size of 0.1mm^3. To induce myocardial damage, processed myocardium pieces were cultured in a cell incubator (at 37 °C and 5% CO2) for 7 days before subsequent culturing.

Isolation of murine embryonic sympathetic ganglia

After resection of the uteri of euthanized pregnant mice, embryos were collected and euthanized in cold PBS. Superior cervical ganglia (SCG) were isolated from E18.5 embryos and kept in cold PBS. Each SCG was processed into 3–4 pieces for subsequent culturing.

Sympathetic ganglion culture and neurite outgrowth assay

Collagen gel was used to provide a 3-dimentional environment for neurite projection from ganglia explants. Freshly isolated SCG explants were randomly cultured under 5 different conditions in complete medium for 6 days before fixation and further staining.

Immunostaining of ganglion explants in gel

All SCG cultured in gel were whole-mount immuno-stained with anti-β-Tubulin III (Tubb3) to visualize outgrowth. Expression of the enzyme Tyrosine hydroxylase (TH), that is part of the catecholamine biosynthesis pathway necessary for stimulating myocardial contraction, was used to demonstrate the sympathetic phenotype of these ganglia [25]. To verify that growing sympathetic SCG were of a similar phenotype as those freshly isolated, whole-mount anti-TH immunostaining was performed in cultured growing SCG as well as in freshly isolated SCG. Growing SCG show a similar TH expression profile as compared to freshly isolated SCG (Supplemental Fig. S2A,B). In addition, post-ganglionic varicosities, the site in the axon were the neurotransmitters are contained and released, forming the site of the synapses [26,27] were detected in our co-cultured ganglionic neurites (Supplemental Fig. S2C).

Quantification of neurite outgrowth

The work flow of outgrowth quantification is illustrated in supplemental Fig. S3A. Tubb3+ images of cultured SCG were used to quantify the neurite outgrowth according to the presence of neurite outgrowth and its directional preference. For directional outgrowth, a method to quantify the length and density of directional neurites was developed based on different existing plugins in ImageJ: briefly, Quadrant picking was used to identify the quadrant showing directional outgrowth towards myocardium/EPDCs; NeuriteJ was utilized to count the directional neurites length and density in this quadrant. To correct for potential differences in amount of myocardium used in each experiment, all data were normalized for myocardial volume. The myocardial volume was measured and calculated by applying z-stack in confocal imaging. The normalized directional neurite outgrowth was calculated as: Normalized directional neurite number = Counted neurite number/ Relative myocardium volume.

PC12 neurite outgrowth assay

Serum-free conditioned media were collected after 48-hour culturing. PC12 cells were cultured in low-serum media (with/without the addition of NGF) or conditioned media supplemented with 1% FBS. After culturing, the PC12 cells were immuno-stained with anti-β-Tubulin III (tubb3) and neurite differentiation of PC12 in each condition was quantified.

Real time PCR and immuno-blotting

Left-ventricular myocardium explants (freshly isolated or cultured for 7 days in vitro) were cultured exclusively or co-cultured with EPDCs for 2 days. Fresh and cultured myocardial explants were collected for gene expression analysis by real time PCR and protein expression analysis by dot blotting and WES (automated Western Blots).

TUNEL assay and immuno-staining in myocardium sections

Sections of freshly isolated, in-vitro cultured (for 7 days) left-ventricular myocardium explants and 7-day post-MI hearts were stained (see Supplement for further details) with TUNEL, anti-NGF and anti-Wilms' tumor 1 (WT-1) antibodies. NGF expression in myocardium explants and post-MI hearts was quantified with ImageJ.

RESULTS

Adult mesenchymal EPDCs enhance neurite outgrowth of sympathetic ganglia

To investigate the relationship of EPDCs with the establishment and remodeling of cardiac sympathetic innervation, murine sympathetic superior cervical ganglia (SCG) of late embryonic

stages (E18.5) were isolated and cultured with human-derived mesenchymal EPDCs in a 3D-culture system. To mimic the in-vivo absence of direct neuron-EPDC communication (cell-cell contact) and determine the paracrine potential, cellular contact between EPDCs and SCG was prevented by preparing the mesenchymal EPDCs as aggregates in collagen gel. In this way, EPDC aggregates were formed, 4 days prior to co-culturing them with E18.5 ganglia in vitro. Each of these EPDC-ganglion co-cultures was allowed to sprout for 6 days, followed by staining to detect the effects of EPDCs on nerve sprouting of SCG in vitro (**Fig. 1A**).

The SCG explants cultured in the vehicle condition (**Fig. 1B**) showed very limited neurite outgrowth, with either absent or very short neurites. SCG explants in +EPDCs condition (**Fig. 1C**) exhibited robust neurite outgrowth with regard to both density and length of neurites. Comparison of the occurrence of neurite outgrowth (regardless of the length and density of neurites) between SCG in vehicle condition and in +EPDCs condition demonstrated that EPDCs significantly increase the neurite outgrowth of sympathetic ganglia (**Fig. 1F**).

Directional sympathetic nerve sprouting is induced by myocardium and this effect is amplified by EPDCs

Communication between target organs and nerve cells contributes to the innervation of target organs [28]. To study whether adult mesenchymal EPDCs participate in facilitating sympathetic neurite sprouting to target tissue (i.e. the heart), ventricular myocardium was included into the co-culture. Adult-derived murine ventricular myocardium explants were prepared and were cultured in-vitro for 7 days prior to co-culture with SCG explants, after which similar procedures were followed as described (**Fig. 1A**). The SCG explants cultured in the +EPDCs+M condition showed not only abundant but also directionally sprouted neurites towards ventricular myocardium explants (**Fig. 1D**) compared to the abundant but non-directional neurite outgrowth of SCG in the +EPDCs condition (**Fig. 1C**).

To clarify the separate roles as well as potential interactions of mesenchymal EPDCs and myocardium affecting ganglionic outgrowth, SCG explants isolated from the same embryos were randomly divided and cultured in either +EPDCs+M or +M conditions. After a matched co-culture period of 6 days, anti-Tubb3 staining showed directionally sprouted neurites towards myocardium explants in both co-culture conditions (**Fig. 1D, E**). However, the sprouting density of neurites appeared higher in the +M+EPDCs compared to the +M group.

When comparing the +M+EPDCs group and the +EPDCs group (**Fig. 1F**), no difference in the total occurrence of outgrowth from the ganglia was detected but neurite outgrowth showed a significant increase in occurrence of directional outgrowth in the +M+EPDCs condition compared to +EPDCs condition (**Fig. 2A**).

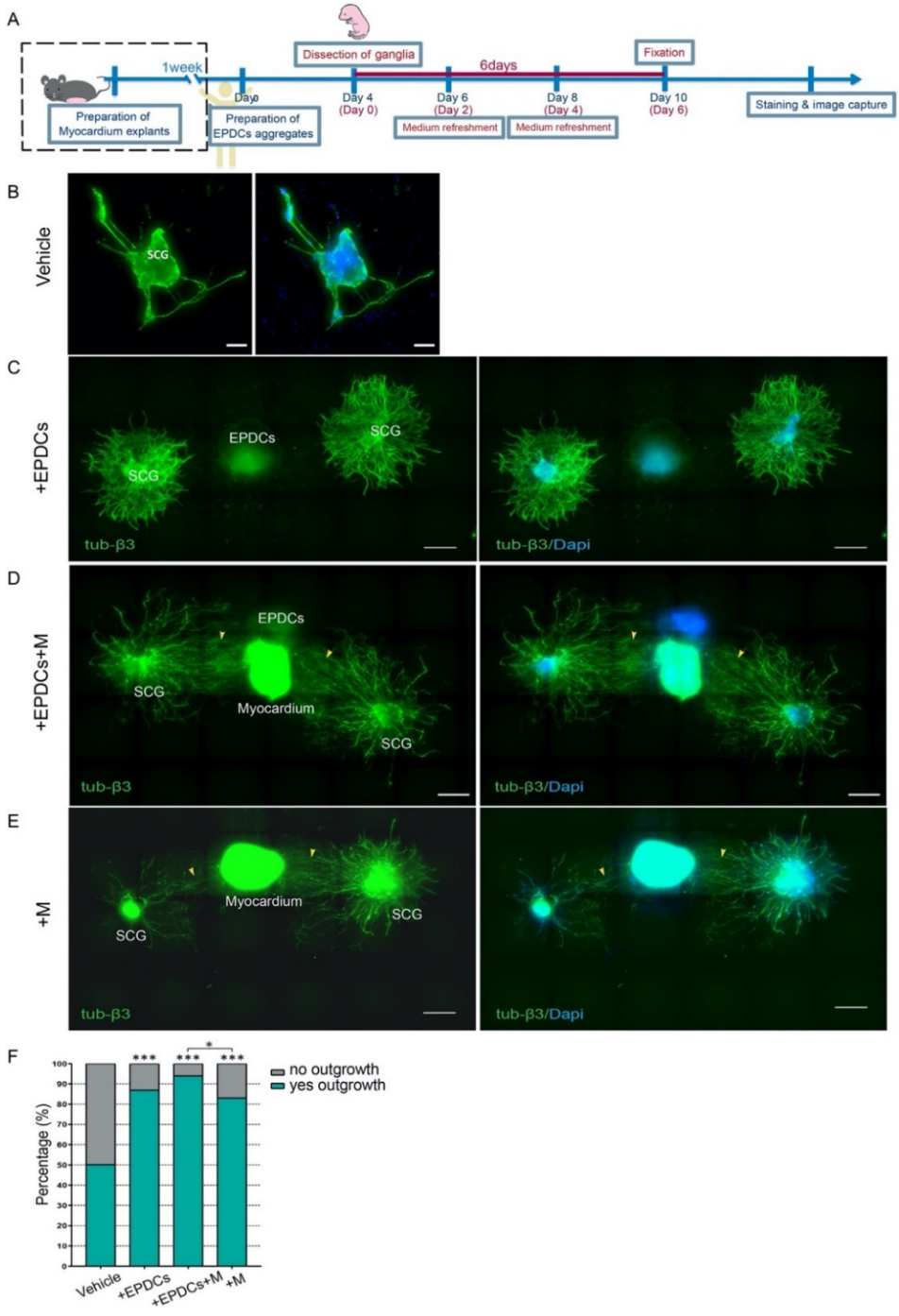
A
1week
Day0
Preparation of Myocardium explants
Preparation of EPDCs aggregates
Dissection of ganglia
6days
Fixation
Day 4 (Day 0)
Day 6 (Day 2)
Day 8 (Day 4)
Day 10 (Day 6)
Medium refreshment
Medium refreshment
Staining & image capture
B
Vehicle
SCG
C
+EPDCs
EPDCs
SCG
SCG
tub-β3
tub-β3/Dapi
D
+EPDCs+M
EPDCs
SCG
Myocardium
SCG
tub-β3
tub-β3/Dapi
E
+M
Myocardium
SCG
SCG
tub-β3
tub-β3/Dapi
F
Percentage (%)
no outgrowth
yes outgrowth
Vehicle
+EPDCs
+EPDCs+M
+M

Fig. 1. Mesenchymal EPDCs enhance the outgrowth of sympathetic ganglia. A. Schematic timeline of events in co-culturing superior cervical ganglia (SCG) with mesenchymal EPDCs or with mesenchymal EPDCs and ventricular myocardium (indicated in the dashed square). B-E. Outgrowth of SCG after 6-days of culturing in indicated conditions. Both EPDCs and cultured ventricular myocardium increase the outgrowth of SCG. Directionally organized neurite outgrowth of SCG (indicated by arrowheads in D and E) are detected in +EPDCs+M (panel D) and +M (panel E) co-culturing conditions. Scale bar represents 100 µm in B and 500 µm in C-E. F. Quantification of the percentage of SCG showing neurite outgrowth shows significant increase of neurite outgrowth in ganglia co-cultured with mesenchymal EPDCs and/or ventricular myocardium as compared to vehicle n = 48 for vehicle condition; n = 38 for +EPDCs condition; n = 96 for +EPDCs+M condition; n = 95 for +M condition. Chi-square test was applied to detect the difference among groups, *P < .05, ***P < .001.

Quantification of neurite density shows significant increase in growth and branching of directional neurites in presence of EPDCs

As a next step the density of directional sprouting of neurites towards myocardium was quantified in both groups (i.e. +M versus +EPDCs +M).

Quadrants in anti-Tubb3 images were determined and #1 was assigned to the quadrant showing neurites outgrowth towards myocardium/EPDCs (supplemental Fig. S3A, Fig. 2B). Outgrowth was designated as “directional outgrowth” when denser and longer neurites were observed in quadrant 1 (as is depicted in the graphs of Supplemental Fig. S3B as red lines). Likewise, neurites sprouting in quadrant 1 were named “directional neurites”. When each quadrant showed a similar neurite density and length, as was the case when SCG were co-cultured with EPDCs only, the outgrowth was designated as “non-directional”. In this case, the colored lines in Supplemental Fig. S3C depicting the different quadrants overlap, as is shown.

Subsequently, once SCG explants in +M+EPDCs and +M conditions showed directional outgrowth, the directional neurites were semi-automatically quantified and normalized for myocardium volume in each corresponding co-culture. The normalized number of directional neurites at each length (from 100 µm to1600 µm) projecting from the SCG explants is shown in a heatmap (Fig. 2C, relative myocardium volume is shown in supplemental Fig. S3D). As is demonstrated in the heat map, directional neurites with high density (red areas) are predominantly encountered in +M+EPDCs condition. Addition of EPDCs also resulted in a significant increase in growth and branching of directional neurites (Fig. 2D).

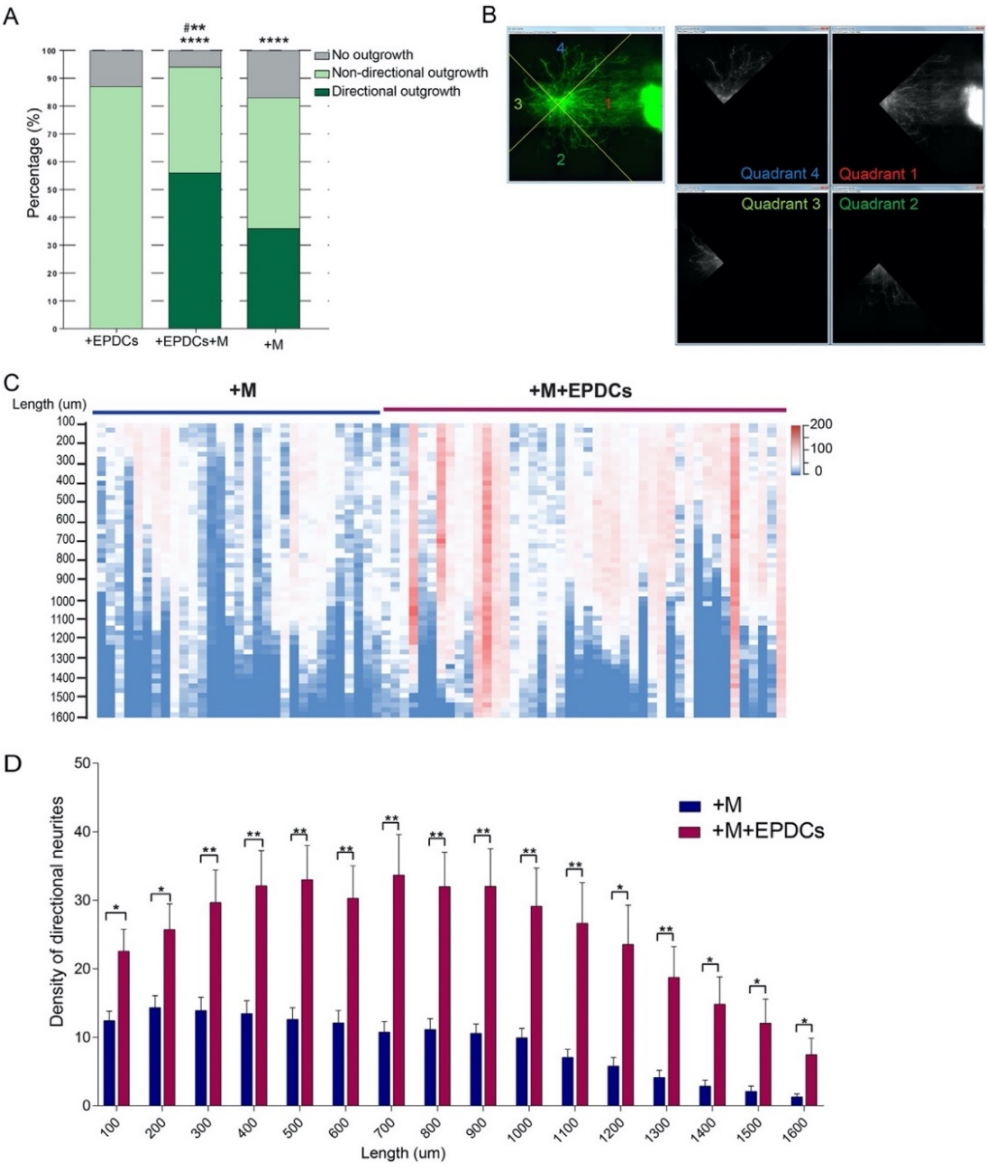

Fig. 2. Mesenchymal EPDCs enhance directional neurite growth of SCG towards ventricular myocardium.
A. Cultured myocardium triggers directional outgrowth (compare +M condition with +EPDCs condition). EPDCs augment this occurrence of directional outgrowth (compare +M condition with +EPDCs+M condition). +EPDC+M condition n = 96, +M condition n = 95. Chi-square test was applied to detect the difference among conditions, **** $p < .0001$ compared to +EPDCs group; #** $p < .01$ compared to +M group. B. To define directional outgrowth, Tubb3+ images with detectable neurite outgrowth were first processed by Quadrant picking in ImageJ, which divided the image in 4 quadrants according to the ganglion-myocardium position (SCG explants shown in Fig. 1D are shown as an example). The quadrants

were numbered 1 to 4, where quadrant 1 is always the one facing the myocardium/EPDC aggregate, followed clockwise by quadrant 2, 3 and 4. C. The normalized density of directional neurites (i.e. the neurites in quadrant 1) at the indicated length is shown as a heatmap. Neurite density increases from blue (lowest density) to dark red (high density). D. Statistical analysis indicates a significant difference of neurite density (y-axis) between directional neurite outgrowth in the +M condition and in the +M+EPDCs condition at each distance (x-axis) (n = 32 for +M group, n = 45 for +M+EPDCs group). Multiple t-test was applied to detect the difference between +M and +M +EPDCs, * $p < .05$, ** $p < .01$.

EPDCs and myocardium augment neurite outgrowth via a paracrine effect

In the SCG/myocardium/EPDC co-cultures, the most dense and elongated neurites were observed in quadrant 1, while outgrowth/ density was less in quadrant 2 and 4 and least in quadrant 3 (supplemental Fig. S3B), suggesting a potential paracrine effect. Therefore, the next experiments used conditioned medium of the different culture groups. PC12 cells, derived from rat adrenal medullary tumor, have been shown as an adequate model to study neurite outgrowth in vitro [29,30]. After exposure to NGF, PC12 cells are induced to switch from a proliferating phenotype to a neuron-like phenotype, i.e. neurite differentiation [31]. Conditioned medium of mesenchymal EPDCs (EPDCs med), ventricular myocardium (M med) and co-cultured myocardium with EPDCs (M+EPDCs med) was collected to study the effect on neurite differentiation of PC12 cells. As PC12 cells need a "trigger" to switch to a differentiating phenotype, the cells were first triggered by exposure to 50 ng/ml NGF followed by culturing in different conditioned mediums to study their outgrowth (Supplemental table 2). All conditioned media could induce clear neurite differentiation of PC12 cells after 2-day triggering with NGF (Fig. 3A). PC12 cells triggered by NGF and subsequently cultured in vehicle medium served as a negative control (NGF+/−) and showed limited neurite differentiation. In contrast, PC12 cells cultured in different conditioned mediums after pre-treatment with NGF showed different degrees of augmentation of neurite differentiation. This was significantly different from the PC12 cells in the negative control (NGF+/−) condition, but comparable to the cells in a positive control (NGF+/+) condition (Fig. 3A,B). Quantification showed a significantly higher neurite differentiation in combined M+EPDCs medium as compared to cells cultured exclusively with either M medium or EPDCs medium (Fig. 3B), in concordance with findings in the SCG co-cultures (Fig. 2D). Culturing PC12 cells with conditioned media without pre-treatment of NGF showed no significant neurite differentiation (Supplemental table 1, Supplemental Fig. S4A).

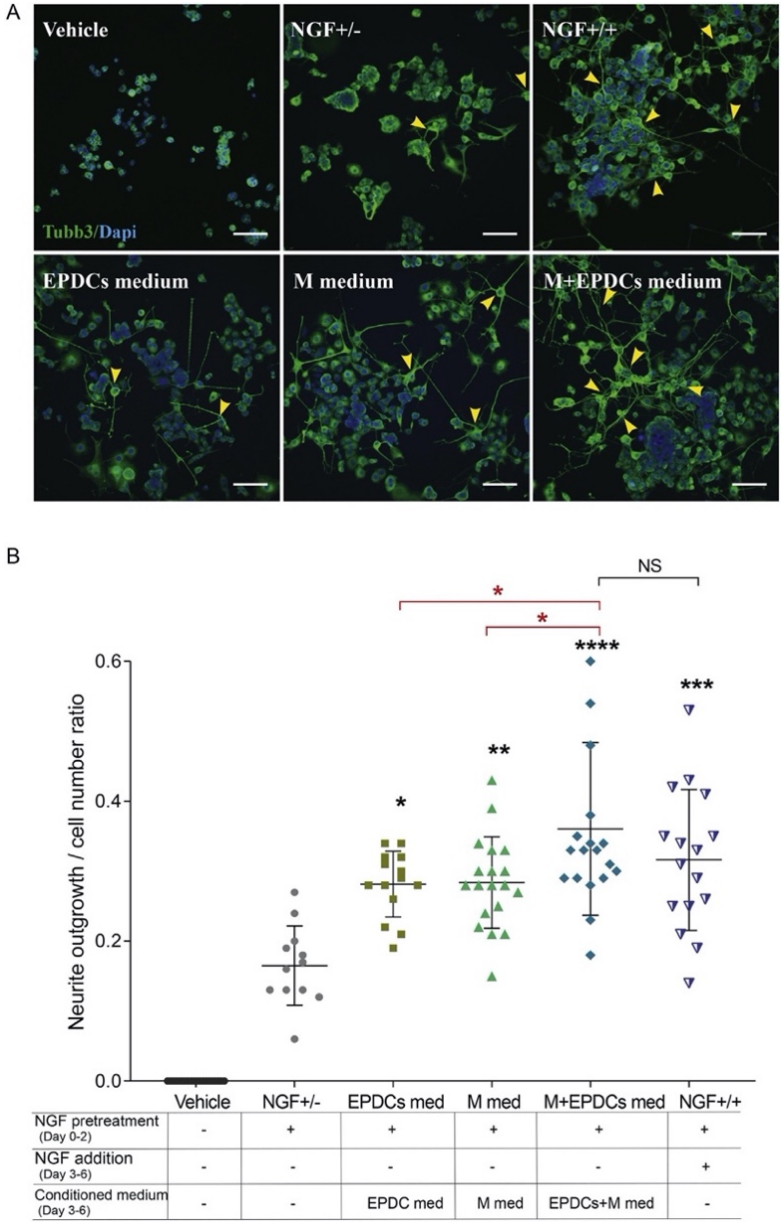

Fig. 3. EPDCs and myocardium augment neurite outgrowth via a paracrine effect. A. Tubb3 staining of PC12 cells cultured under different conditions as indicated (also see supplemental Table 2). Differentiated PC12 cells and neurites are indicated by arrow heads. Scale bar = 100μm. B. Neurite outgrowth of PC12 cells cultured in the indicated conditions (shown in the table below the graph) is

quantified and displayed as mean ± SD. One-way ANOVA was applied to detect differences in neurite outgrowth among conditions, and Post Hoc Test (Tukey's multiple comparisons test) in one-way ANOVA was performed to detect the specific difference between groups, * p < .05, ** p < .01, *** p< .001 **** p < .0001 compared to NGF+/− condition.

EPDCs increase the expression of NGF in cultured myocardium compared to fresh myocardium

In contrast to the robust neurite sprouting of SCG co-cultured with pre-cultured myocardium, co-culturing SCG with freshly isolated myocardium (+fresh M), showed strikingly less directional outgrowth and only limited density of directional neurites (Fig. 4A). TUNEL assay revealed apoptosis in cultured myocardium but not in freshly isolated myocardium. (Fig. 5A, B). Hif1a (hypoxia-inducible factor 1-alpha), known to regulate the cellular and systemic homeostatic response to hypoxia and activate genes involving energy metabolism and apoptosis, plays a critical role in adaption of ischemic disease [32,33]. Its expression was increased in the ex-vivo cultured myocardium explants, especially in the myocardium co-cultured with EPDCs (Supplemental Fig. S4B). This led to the hypothesis that cultured myocardium explants might show signs of ischemia related cell death leading to the release of factors stimulating neuronal outgrowth. Therefore as a next step several neurotrophic factors known to induce innervation, including *Gdnf*, *Ntf3* and *Igfbp6* were examined by RT-PCR, but were not significantly changed in cultured myocardium. The expression of these genes was not significantly altered by the presence of EPDCs either (Supplemental Fig. S4B). However, expression of other genes, like *Bmp2*, *Fgf2*, *Tgfb1* and *Tgfb3* was significantly increased in cultured myocardium (Supplemental Fig. S4B). These genes are known to be involved in various events including cardiac development (i.e. epicardial EMT and differentiation), angiogenesis, neuron differentiation/growth and peripheral nerve regeneration.

In addition to the neurotrophic factors mentioned above, expression of NGF was studied, as it is one of the most critical factors for neuronal survival and nerve growth and has been shown to increase under hypoxic conditions and is released acutely from ischemic myocardium [34,35]. Its induction is regulated by ET-1 via the endothelin receptor A (ETA), which participates in cardiac sympathetic nerve growth during development [36]. As we previously found an increase of ET-1 in re-activated mesenchymal human EPDCs (Supplemental Fig. S4C), we first examined the expression of gene Endothelin receptor A (*EdnrA*) in myocardium. Increased EdnrA expression was observed in cultured myocardium as compared to fresh isolated myocardium (Fig. 4B). As a next step, NGF expression in cultured versus fresh myocardium was examined by real time PCR. Results showed that NGF in cultured myocardium was significantly upregulated compared to fresh isolated myocardium (Fig. 4B). SEMA3A, a chemorepellent of axonal outgrowth critical for the formation of normal cardiac innervation, was also examined and a decline of SEMA3A expression was detected in the cultured

myocardial tissue at mRNA level (**Fig. 4B**). Both NGF and SEMA3A were further confirmed at protein level by WES (automated Western Blotting) and showed more outspoken alterations in cultured myocardium at protein level (**Fig. 4C, D**). After co-culturing of myocardium explants with EPDCs, NGF protein was further upregulated in myocardium explants (**Fig. 4C**).

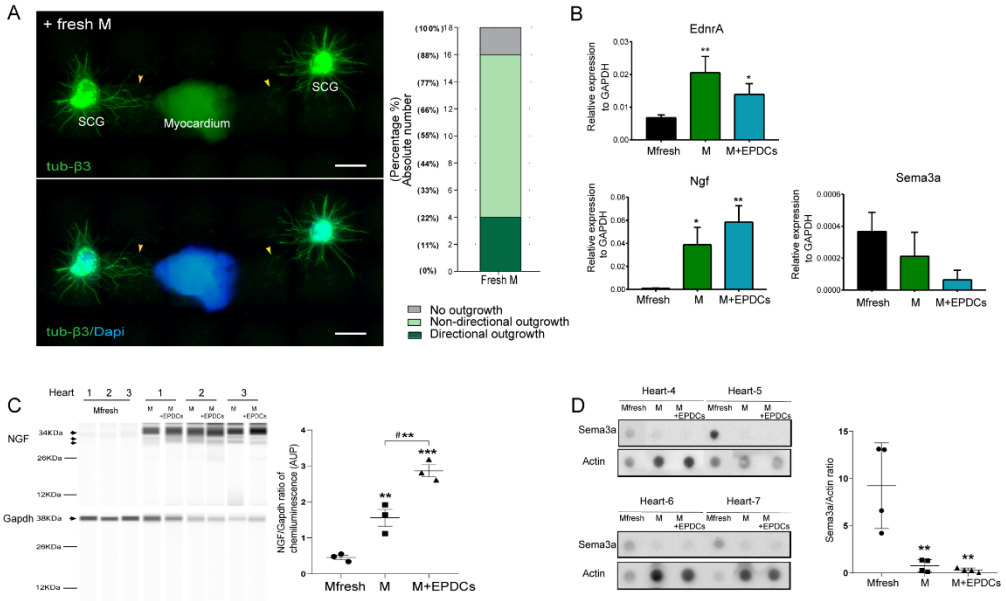

Fig. 4. EPDCs increase the expression of neurotrophic factors in cultured myocardium. A. SCG co-cultured with freshly isolated myocardium explants (left panel) and the quantification of outgrowth (right panel). Directional neurite outgrowth is indicated with arrowheads. Scale bar = 500µm. B. Real time PCR results of *Ngf*, *Sema3a* and *EdnrA* expression in freshly isolated myocardium, cultured myocardium and myocardium co-cultured with EPDCs (n = 6). Mfresh = freshly isolated myocardium; Mculture = cultured myocardium ** p < .01 compared to Mfresh. C. The expression of NGF protein in cultured myocardium and in myocardium co-cultured with EPDCs (n = 3), determined by WES (automated western blots). Mfresh = freshly isolated myocardium; M = cultured myocardium; M+EPDCs = the myocardium co-cultured with EPDCs. *p < .05, ** p < .01 compare to Mfresh, #** p < .01 compared to M+EPDCs with M. D. SEMA3A protein in myocardium explants as determined by dot-blotting (n = 4). * p < .05, ** p < .01 compared to Mfresh. Mfresh = freshly isolated myocardium; M = cultured myocardium; M+EPDCs = the myocardium co-cultured with EPDCs. One-way ANOVA and Post Hoc Test (Tukey's multiple comparison test) were performed to detect the differences.

To confirm the finding of NGF at the tissue level, fresh and cultured myocardial explants as well as explants co-cultured with EPDCs from the same mouse were sectioned and stained

with anti-NGF antibody. In fresh myocardium, only a very limited amount of anti-NGF staining was detected (**Fig. 5C**). In cultured myocardium however, robust staining of NGF was detected, mainly observed in non-cardiomyocyte cells, like cells in vessels with slightly increased NGF detection in cardiomyocytes (**Fig. 5D**). The presence of EPDCs, as is shown in **Fig. 5E**, further increased the expression of NGF, which could be widely detected in both cardiomyocytes and non-cardiomyocytes of cultured myocardium. To compare with the in-vivo situation, sections of cardiac tissue after myocardial infarction were studied (**Fig. 6**). As expected, activation of epicardium was observed with expression of WT-1 in the epicardium (**Fig. 6A,B**) as reported previously [20]. In the ischemic zone, NGF expression was observed in cardiomyocytes and non-cardiomyocytes including the activated epicardial cells, similar to the findings in myocardium explants co-cultured with EPDCs in vitro (**Fig. 6C**). In contrast, in the area remote from the infarction, only a low amount of NGF expression was observed similar to the pattern in fresh isolated healthy myocardium explants (**Fig. 6D,E**), supporting a role of EPDCs on upregulation of NGF in "damaged" myocardium. Quantification of NGF protein confirmed an significant increase in both the myocardial explants co-cultured with EPDCs and in the ischemic area of post-MI hearts (**Fig. 6F, G**).

(Figure 5 is on the next page)

Fig. 5. Cultured myocardium explants shows apoptosis and expression of NGF. A-B. Detection of apoptosis in fresh and 7-day cultured myocardium explants with TUNEL assay. Scale bar = 100µm. C-E. Anti-NGF staining in fresh myocardium explants, in cultured myocardium explants and in myocardium explants co-cultured with EPDCs. Anti-Tropomyosin was performed to label cardiomyocytes. Arrowheads indicate cardiomyocytes with NGF staining of high intensity. Dash lined-circles indicate vessels. Scale bar = 100µm.

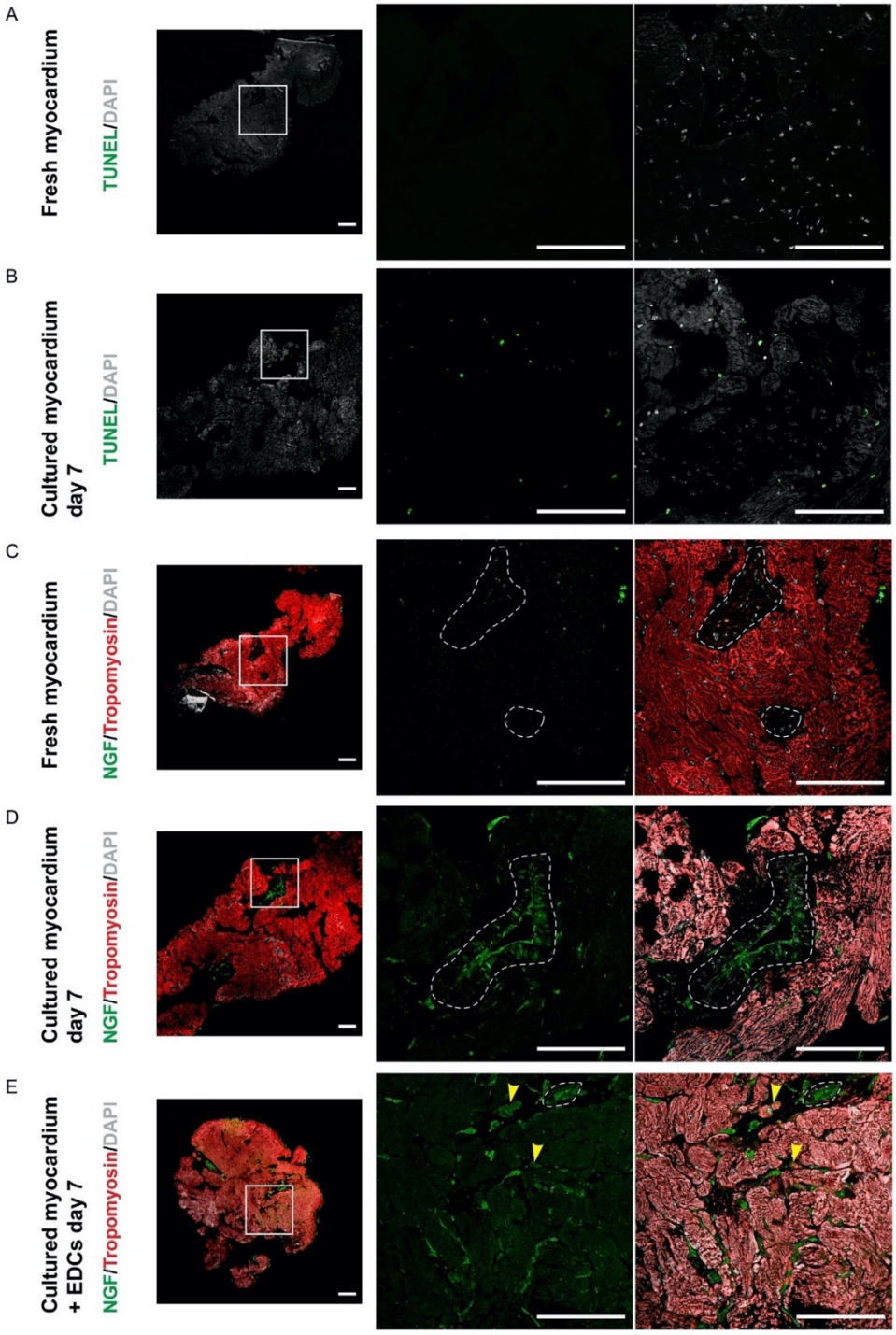
A
Fresh myocardium
TUNEL/DAPI
B
Cultured myocardium
day 7
TUNEL/DAPI
C
Fresh myocardium
NGF/Tropomyosin/DAPI
D
Cultured myocardium
day 7
NGF/Tropomyosin/DAPI
E
Cultured myocardium
+ EDCs day 7
NGF/Tropomyosin/DAPI

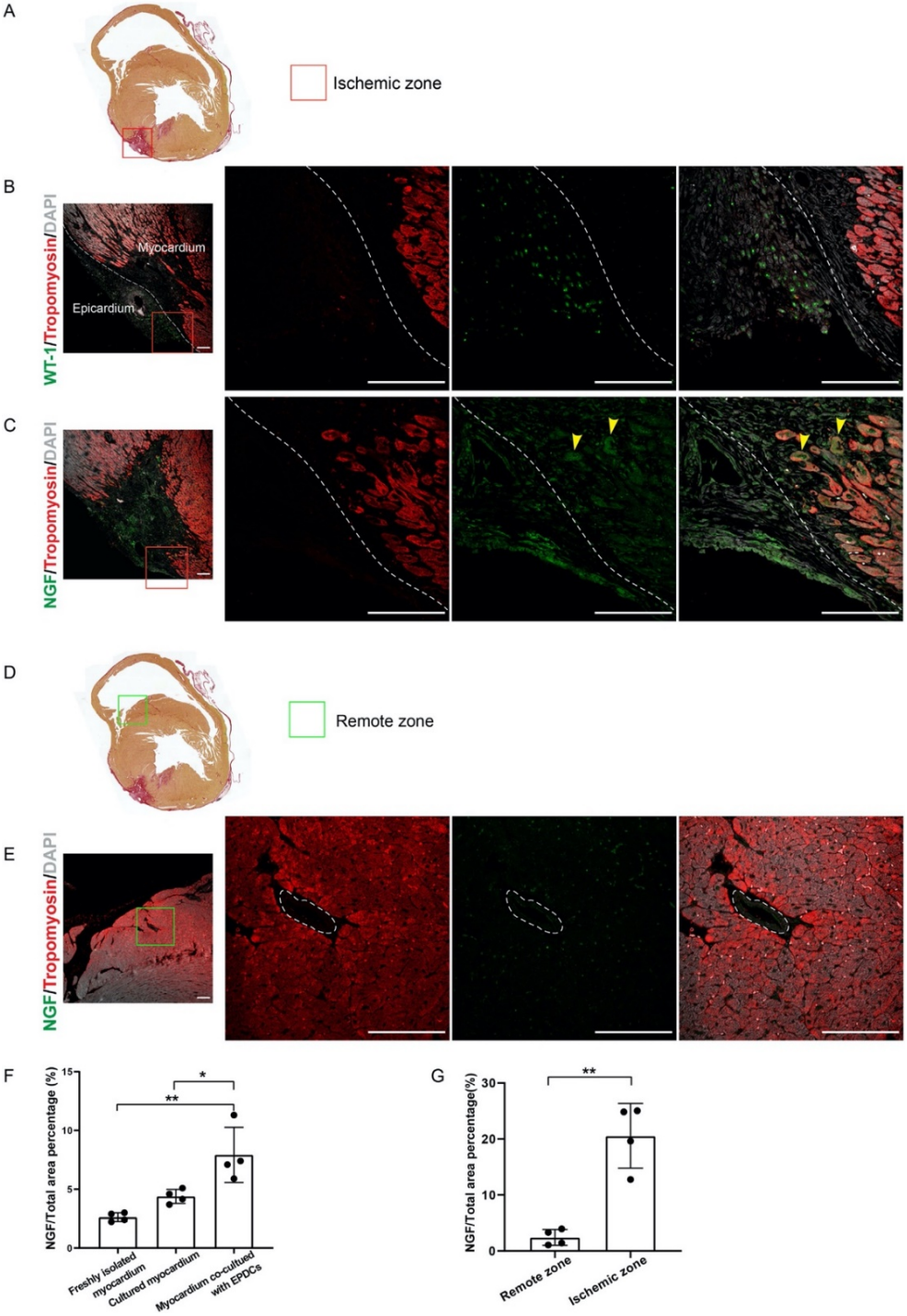
A
Ischemic zone
B
WT-1/Tropomyosin/DAPI
Myocardium
Epicardium
C
NGF/Tropomyosin/DAPI
D
Remote zone
E
NGF/Tropomyosin/DAPI
F
NGF/Total area percentage (%)
Freshly isolated myocardium
Cultured myocardium
Myocardium co-cultued with EPDCs
G
NGF/Total area percentage(%)
Remote zone
Ischemic zone

Fig. 6. Expression of NGF at Ischemic zone of infarcted heart. A,D Sirius red staining of infarcted murine heart (7 days after ligation of the left anterior descending coronary artery). The red square indicates the ischemic zone shown in B and C. B. Activation of epicardium in the infarcted murine heart with the re-expression of WT-1 in epicardial cells. The dashed line indicates the borderline of epicardium at ischemic zone. Scale bar = 100µm. C. Anti-NGF and anti-tropomyosin staining of the ischemic zone. Arrowheads indicate cardiomyocytes with NGF staining of high intensity. The dashed line indicates the borderline of epicardium at the ischemic zone. Scale bar = 100µm. D, E. Anti-NGF and anti-tropomyosin staining of remote zone. The dash lined-circle indicates the vessel. Scale bar = 100µm. D. Sirius red staining of the infarcted murine heart (7 days after ligation of the left anterior descending coronary artery). The green square indicates the remote (un-infarcted) zone shown in E. E. Anti-NGF and anti-tropomyosin staining of the remote (un-infarcted zone). The dash lined-circle indicates the vessel. F. Quantification of NGF expression in freshly isolated myocardium, cultured myocardium and the myocardium co-cultured with EPDCs in vitro for 7 days (n = 4). G. Quantification of NGF expression at ischemic zone and remote zone of ischemic murine hearts (n = 4). * P < .05, ** P < .01.

DISCUSSION

Ventricular tachyarrhythmias secondary to myocardial infarction (MI) are a major risk factor for sudden cardiac death and have been increasingly associated with ventricular sympathetic hyperinnervation [7,37]. For ventricular (hyper)innervation to occur, axons must grow out of sympathetic chain ganglia towards the heart [11]. Likely, factors from the heart in response to ischemia/hypoxia cause retrograde stimulation of ganglia to induce axonal outgrowth [38]. In the current study, we aimed to explore a potential role of EPDCs in this process.

The epicardium is composed of multifunctional, multipotent progenitor cells with important roles during fetal development [14,15,39]. Of interest, the fetal epicardium transiently expresses the autonomic β2-adrenergic receptor, and the presence of this mono-layer on the surface of the myocardium was shown to be essential for the early autonomic response [19]. However, whether and how epicardium or EPDCs participate in the establishment of cardiac sympathetic innervation, especially in the remodeling of sympathetic innervation in states of cardiac damage is largely unknown. Although mesenchymal EPDCs are able to differentiate into several cell types, including cardiac fibroblasts, which have been suggested to induce cardiac sympathetic hyperinnervation after MI [40], there is no direct evidence linking EPDCs to sympathetic innervation, as yet.

During development, cardiac autonomic ganglia and nerve fibers have their origin in the neural crest [41], multipotent cells that derive from the embryonic neural plate. Ventricular autonomic innervation develops in parallel with ventricular vascularization, guided by neurotrophic factors [12]. In the current study, in which we co-cultured mouse sympathetic chain ganglia with myocardium and human EPDCs in a collagen based 3D co-culture system, we found evidence for a role of EPDCs in stimulating neuronal outgrowth. This observation opens up a novel approach to understanding of the regulation of the autonomic innervation

of the heart. In all circumstances, adding EPDCs to the ganglion cultures induced a synergistic effect as compared to culturing ganglia with either EPDCs or myocardium alone. The mutual interaction between myocardium and EPDCs has been demonstrated by our group as well in other circumstances, where EPDCs influenced for instance the proper maturation and alignment of myocardium [18,42].

The question remains why healthy murine ganglia, started to show an increase in outgrowth in our in vitro culturing model. We postulated that ischemia/hypoxia induced conditions mimicked a condition of cardiac damage. This was supported by the ganglia-EPDC co-cultures with fresh myocardium, that showed remarkably less outgrowth. These findings are in line with observations in other cell culture systems, showing that even concentrations of oxygen in the physiological range may exert a significant negative impact on cells in culture [43]. Our data on the possible role of induction of "cardiac damage" was further supported by the increase of levels of Hypoxia-inducible factor 1-alpha (*Hif1a*) in cultured myocardial cells, already starting after 1 day of culture. *Hif1a* is known to regulate the cellular and systemic homeostatic response to hypoxia and activate genes involving energy metabolism and apoptosis, and plays a critical role in adaption to ischemic disease [32,33].

Paracrine effect of mesenchymal EPDCs on neurite outgrowth. The current culturing experiments using PC12 cells cultured with conditioned media of myocardium, EPDCs and both, confirmed a paracrine effect of EPDCs on the differential potential of neurons. PC12 cells are derived from rat adrenal medullary tumor cells and have been shown an adequate model to study neurite outgrowth in vitro [29,30]. In line with the in vitro results of ganglion cultures, a synergistic effect of the addition of EPDC medium to the PC12 cell culture was observed, with an increase in neurite sprouting as compared to cultures with either myocardium or EPDCs medium alone. It is well established that epicardium and its EPDCs exert effects on the heart through paracrine signaling via secreted factors [44], which is considered crucial in the regenerative role of EPDCs after MI [16], although a potential effect on neuronal outgrowth has not been described to date. Interestingly, comparable like the in vivo situation after MI, where neurons only start growing fast after an "ischemic hit", PC12 cells are in a "default" dormant proliferating state and only start differentiating and sprouting when triggered by addition of NGF. NGF is a critical neurotrophic factor supporting neuron survival and axonal growth. Levels of myocardial NGF increased substantially in the presence of EPDCs, demonstrated at both mRNA and protein level. NGF has two main isotypes in vivo; it is initially synthesized as a precursor, proNGF (a complex of alpha, beta and gamma unit) and can be cleaved into a mature functional beta NGF [45]. We only found a low amount of mature NGF staining in fresh myocardium, consistent with a previous report describing the absence of mature NGF in most healthy tissues in both mouse and human [46]. In vivo, anti-mature NGF

staining in epicardium-activated hearts (7-day post-MI) supported our findings that EPDCs increase the NGF expression in both non-cardiomyocyte cells as well as in cardiomyocytes in the myocardium.

Similar results in our study were found for other factors involved in regulation of cardiac innervation. Endothelin 1, increasing cardiac innervation via NGF in animal models [36], was upregulated in myocardium in the presence of EPDCs. In contrast, axonal repellent factor, SEMA3A, that guides the establishment of normal epicardium-to-endocardium cardiac sympathetic innervation [47], was decreased in cultured myocardium, the effect of which was again augmented by the presence of mesenchymal EPDCs. This decrease in SEMA3 expression could underline an increased potential for neuronal growth, as SEMA3A has a suppressive function on neuronal growth [48]. Conversely, overexpression of SEMA3A in either the ischemic border zone of myocardium or in sympathetic ganglia was able to diminish cardiac sympathetic hyperinnervation in the damaged heart [47,49].

Besides a modulation of myocardial NGF and SEMA3A expression by EPDCs, an upregulation of transcriptional expression of *Bmp2*, *Fgf2*, *Tgfb1* and *Tgfb3* was also detected. These genes have various functions including their role as growth factors for multiple cell types, participating in cardiac development, directing cells differentiation, as well as promoting peripheral nerve regeneration [50–53].

STUDY LIMITATIONS

Murine ganglia and myocardium were cultured with human adult EPDCs. In an ideal setting tissues of the same species (preferably human) would be used. The use of our setup was partly directed by the difficulties encountered of culturing murine EPDCs in vitro. In addition, acquiring fresh ventricular human tissues and ganglia suitable for prolonged culture is challenging. On the other hand, the use of human cells is beneficial from a translational point of view. In other studies we also successfully cultured murine and human tissues [22,54], as was also reported by other researchers [55].

As EPDCs are derived from human adult cells, obtained as anonymous surplus operation tissues, we were blinded to any patient information. This may explain some of the variations we encountered in our cell cultures. In the future, we strive to obtained immortalized/ clonal cell lines, that would provide a solution for these interindividual variations. On the other hand, the current study more closely mimics the situation encountered in clinical settings, were individuals factor will always play a role in outcome.

CONCLUSIONS AND CLINICAL PERSPECTIVE

In conclusion, in the current paper we propose a new role for EPDCs extending their potential role in cardiac regeneration in states of ischemia to include an effect on cardiac (re)innervation. Because of its complexity, the autonomic nervous system is in many respects still enigmatic and the pathways regulating neural growth and differentiation, especially in disease states are complex and largely unresolved. We show that the promotional effect of mesenchymal EPDCs on sympathetic neurite sprouting is via paracrine signaling, and indicate a role of NGF, Endothelin-1 and SEMA3A in the process. This response may be in essence beneficial in vivo, restoring loss of functional nerves after damage, but given the occurrence of hyperinnervation-related lethal arrhythmias, an "overshoot" may occur, with adverse effect on prognosis after cardiac damage. Which of those factors released by the ventricular myocardium and/or EPDCs are crucial in promoting nerve outgrowth, requires further exploration including metabolomics/proteomics. Our findings warrant more extensive molecular studies, aimed at exploring the neural-myocardial-epicardial axis such as RNA sequencing of ganglionic, myocardial and epicardial tissues in normal and disease states, exploring other signaling pathways involved.

ACKNOWLEDGEMENTS

We thank T. van Herwaarden and Esther Dronkers (Department of Cell and Chemical Biology, LUMC, Leiden, the Netherlands) for their help with isolating and culturing of human EPDCs, and A. Végh (Department of Cell and Chemical Biology, LUMC, Leiden, the Netherlands) for technical assistance.

REFERENCES

[1] M. Vaseghi, J. Gima, C. Kanaan, O.A. Ajijola, A. Marmureanu, A. Mahajan, et al. Cardiac sympathetic denervation in patients with refractory ventricular arrhythmias or electrical storm: intermediate and long-term follow-up, Heart Rhythm 11(3) (2014) 360-6.
[2] M.J. Shen, D.P. Zipes, Role of the autonomic nervous system in modulating cardiac arrhythmias, Circ Res 114(6) (2014) 1004-21.
[3] D.P. Zipes, M. Rubart, Neural modulation of cardiac arrhythmias and sudden cardiac death, Heart Rhythm 3(1) (2006) 108-13.
[4] M. Vaseghi, K. Shivkumar, The role of the autonomic nervous system in sudden cardiac death, Prog Cardiovasc Dis 50(6) (2008) 404-19.
[5] J.M.T. Debakker, F.J.L. Vancapelle, M.J. Janse, S. Tasseron, J.T. Vermeulen, N. Dejonge, J.R. Lahpor, Slow Conduction in the Infarcted Human Heart - Zigzag Course of Activation, Circulation 88(3) (1993) 915-926.
[6] T. Yokoyama, J.K. Lee, K. Miwa, T. Opthof, S. Tomoyama, H. Nakanishi, A. Yoshida, et al. Quantification of sympathetic hyperinnervation and denervation after myocardial infarction by three-dimensional assessment of the cardiac sympathetic network in cleared transparent murine hearts, PLoS One 12(7) (2017) e0182072.
[7] C.Y. Li, Y.G. Li, Cardiac Sympathetic Nerve Sprouting and Susceptibility to Ventricular Arrhythmias after Myocardial Infarction, Cardiol Res Pract 2015 (2015) 698368.
[8] T.M. Lee, C.C. Chen, N.C. Chang, Cardiac sympathetic hyperinnervation in deoxycorticosterone acetate-salt hypertensive rats, Clin Sci (Lond) 123(7) (2012) 445-57.
[9] K. Kimura, M. Ieda, H. Kanazawa, T. Yagi, M. Tsunoda, S. Ninomiya, H. Kurosawa, K. Yoshimi, H. Mochizuki, K. Yamazaki, S. Ogawa, K. Fukuda, Cardiac sympathetic rejuvenation: a link between nerve function and cardiac hypertrophy, Circ Res 100(12) (2007) 1755-64.
[10] Y.S. Oh, A.Y. Jong, D.T. Kim, H.M. Li, C. Wang, A. Zemljic-Harpf, et al. Spatial distribution of nerve sprouting after myocardial infarction in mice, Heart Rhythm 3(6) (2006) 728-736.
[11] T. Kawashima, The autonomic nervous system of the human heart with special reference to its origin, course, and peripheral distribution, Anat Embryol 209(6) (2005) 425-438.
[12] J. Nam, I. Onitsuka, J. Hatch, Y. Uchida, S. Ray, S. Huang, W. Li, H. Zang, P. Ruiz-Lozano, Y.S. Mukouyama, Coronary veins determine the pattern of sympathetic innervation in the developing heart, Development 140(7) (2013) 1475-85.
[13] E. Manousiouthakis, M. Mendez, M.C. Garner, P. Exertier, T. Makita, Venous endothelin guides sympathetic innervation of the developing mouse heart, Nature Communications 5 (2014).
[14] A.C. Gittenberger-de Groot, E.M. Winter, M.M. Bartelings, M.J. Goumans, M.C. DeRuiter, R.E. Poelmann, The arterial and cardiac epicardium in development, disease and repair, Differentiation 84(1) (2012) 41-53.
[15] N. Smart, K.N. Dube, P.R. Riley, Epicardial progenitor cells in cardiac regeneration and neovascularisation, Vascul Pharmacol 58(3) (2013) 164-73.
[16] A.M. Smits, E. Dronkers, M.J. Goumans, The epicardium as a source of multipotent adult cardiac progenitor cells: Their origin, role and fate, Pharmacol Res 127 (2018) 129-140.
[17] A. von Gise, W.T. Pu, Endocardial and Epicardial Epithelial to Mesenchymal Transitions in Heart Development and Disease, Circ Res 110(12) (2012) 1628-1645.
[18] E.A.F. Mahtab, M.C.E.F. Wijffels, N.M.S. Van den Akker, N.D. Hahurij, H. Lie-Venema, L.J. Wisse, M.C. DeRuiter, et al. Cardiac malformations and myocardial abnormalities in Podoplanin knockout mouse embryos: Correlation with abnormal epicardial development, Dev Dynam 237(3) (2008) 847-857.

[19] T.P. Kelder, S.N. Duim, R. Vicente-Steijn, A.M.D. Vegh, B.P.T. Kruithof, A.M. Smits, et al. The epicardium as modulator of the cardiac autonomic response during early development, Journal of Molecular and Cellular Cardiology 89 (2015) 251-259.
[20] A.C. Gittenberger-de Groot, E.M. Winter, R.E. Poelmann, Epicardium-derived cells (EPDCs) in development, cardiac disease and repair of ischemia, J Cell Mol Med 14(5) (2010) 1056-1060.
[21] E.M. Winter, A.C. Gittenberger-de Groot, Epicardium-derived cells in cardiogenesis and cardiac regeneration, Cell Mol Life Sci 64(6) (2007) 692-703.
[22] E.M. Winter, R.W. Grauss, B. Hogers, J. van Tuyn, R. van der Geest, H. Lie-Venema, et al. Preservation of left ventricular function and attenuation of remodeling after transplantation of human epicardium-derived cells into the infarcted mouse heart, Circulation 116(8) (2007) 917-927.
[23] E. Dronkers, A.T. Moerkamp, T. van Herwaarden, M.J. Goumans, A.M. Smits, The Isolation and Culture of Primary Epicardial Cells Derived from Human Adult and Fetal Heart Specimens, Jove-J Vis Exp (134) (2018).
[24] A.T. Moerkamp, K. Lodder, T. van Herwaarden, E. Dronkers, C.K.E. Dingenouts, F.C. Tengstrom, T.J. van Brakel, et al. Human fetal and adult epicardial-derived cells: a novel model to study their activation, Stem Cell Res Ther 7 (2016).
[25] R.E. Zigmond, Y. Ben-Ari, Electrical stimulation of preganglionic nerve increases tyrosine hydroxylase activity in sympathetic ganglia, Proc Natl Acad Sci U S A 74(7) (1977) 3078-80.
[26] V. Prando, F. Da Broi, M. Franzoso, A.P. Plazzo, N. Pianca, M. Francolini, et al. Dynamics of neuroeffector coupling at cardiac sympathetic synapses, J Physiol-London 596(11) (2018) 2055-2075.
[27] M.R. Bennett, A. Cheung, K.L. Brain, Sympathetic neuromuscular transmission at a varicosity in a syncytium, Microsc Res Techniq 42(6) (1998) 433-450.
[28] M.E. Schwab, R. Heumann, H. Thoenen, Communication between Target Organs and Nerve-Cells - Retrograde Axonal-Transport and Site of Action of Nerve Growth-Factor, Cold Spring Harb Sym 46 (1981) 125-134.
[29] L.A. Greene, A.S. Tischler, Establishment of a Noradrenergic Clonal Line of Rat Adrenal Pheochromocytoma Cells Which Respond to Nerve Growth-Factor, P Natl Acad Sci USA 73(7) (1976) 2424-2428.
[30] N.M. Radio, W.R. Mundy, Developmental neurotoxicity testing in vitro: Models for assessing chemical effects on neurite outgrowth, Neurotoxicology 29(3) (2008) 361-376.
[31] S.C. Kao, R.K. Jaiswal, W. Kolch, G.E. Landreth, Identification of the mechanisms regulating the differential activation of the MAPK cascade by epidermal growth factor and nerve growth factor in PC12 cells, J Biol Chem 276(21) (2001) 18169-18177.
[32] G.L. Semenza, Hypoxia-Inducible Factor 1 and Cardiovascular Disease, Annu Rev Physiol 76 (2014) 39-56.
[33] G.L. Semenza, Hypoxia-inducible factor 1: Regulator of mitochondrial metabolism and mediator of ischemic preconditioning, Bba-Mol Cell Res 1813(7) (2011) 1263-1268.
[34] J.O. Hiltunen, A. Laurikainen, A. Vakeva, S. Meri, M. Saarma, Nerve growth factor and brain-derived neurotrophic factor mRNAs are regulated in distinct cell populations of rat heart after ischaemia and reperfusion, J Pathol 194(2) (2001) 247-53.
[35] T. Abe, D.A. Morgan, D.D. Gutterman, Protective role of nerve growth factor against postischemic dysfunction of sympathetic coronary innervation, Circulation 95(1) (1997) 213-220.
[36] M. Ieda, K. Fukuda, Y. Hisaka, K. Kimura, H. Kawaguchi, J. Fujita, K. Shimoda, E. Takeshita, et al. Endothelin-1 regulates cardiac sympathetic innervation in the rodent heart by controlling nerve growth factor expression, J Clin Invest 113(6) (2004) 876-884.
[37] K. Fukuda, H. Kanazawa, Y. Aizawa, J.L. Ardell, K. Shivkumar, Cardiac Innervation and Sudden Cardiac Death, Circulation Research 116(12) (2015) 2005-2019.

[38] G.W. O'Keeffe, H. Gutierrez, L. Howard, C.W. Laurie, C. Osorio, N. Gavalda, S.L. Wyatt, A.M. Davies, Region-specific role of growth differentiation factor-5 in the establishment of sympathetic innervation, Neural Dev 11 (2016).
[39] A. Wessels, J.M. Perez-Pomares, The epicardium and epicardially derived cells (EPDCs) as cardiac stem cells, Anat Rec Part A 276a(1) (2004) 43-57.
[40] C. Mias, C. Coatrieux, C. Denis, G. Genet, M.H. Seguelas, N. Laplace, et al. Cardiac Fibroblasts Regulate Sympathetic Nerve Sprouting and Neurocardiac Synapse Stability, Plos One 8(11) (2013) e79068.
[41] R. Lumb, Q. Schwarz, Sympathoadrenal neural crest cells: the known, unknown and forgotten?, Dev Growth Differ 57(2) (2015) 146-57.
[42] A. Weeke-Klimp, N.A.M. Bax, A.R. Bellu, E.M. Winter, J. Vrolijk, J. Plantinga, S. Maas, M. Brinker, et al. Epicardium-derived cells enhance proliferation, cellular maturation and alignment of cardiomyocytes, Journal of Molecular and Cellular Cardiology 49(4) (2010) 606-616.
[43] A.K. Balin, A.J. Fisher, M. Anzelone, I. Leong, R.G. Allen, Effects of establishing cell cultures and cell culture conditions on the proliferative life span of human fibroblasts isolated from different tissues and donors of different ages, Exp Cell Res 274(2) (2002) 275-287.
[44] M. Masters, P.R. Riley, The epicardium signals the way towards heart regeneration, Stem Cell Res 13(3) (2014) 683-692.
[45] B. Bax, T.L. Blundell, J. MurrayRust, N.Q. McDonald, Structure of mouse 7S NGF: a complex of nerve growth factor with four binding proteins, Structure 5(10) (1997) 1275-1285.
[46] M. Fahnestock, G. Yu, M.D. Coughlin, ProNGF: a neurotrophic or an apoptotic molecule?, Prog Brain Res 146 (2004) 101-10.
[47] R.H. Chen, Y.G. Li, K.L. Jiao, P.P. Zhang, Y. Sun, L.P. Zhang, et al. Overexpression of Sema3a in myocardial infarction border zone decreases vulnerability of ventricular tachycardia post-myocardial infarction in rats, J Cell Mol Med 17(5) (2013) 608-16.
[48] T. Toyofuku, J. Yoshida, T. Sugimoto, H. Zhang, A. Kumanogoh, M. Hori, et al. FARP2 triggers signals for Sema3A-mediated axonal repulsion, Nat Neurosci 8(12) (2005) 1712-1719.
[49] L.C. Yang, P.P. Zhang, X.M. Chen, C.Y. Li, J. Sun, J.W. Hou, et al. Semaphorin 3a transfection into the left stellate ganglion reduces susceptibility to ventricular arrhythmias after myocardial infarction in rats, Europace 18(12) (2016) 1886-1896.
[50] T. Schlange, B. Andree, H.H. Arnold, T. Brand, BMP2 is required for early heart development during a distinct time period, Mech Develop 91(1-2) (2000) 259-270.
[51] Y. Morikawa, A. Zehir, E. Maska, C.X. Deng, M.D. Schneider, Y. Mishina, et al. BMP signaling regulates sympathetic nervous system development through Smad4-dependent and -independent pathways, Development 136(21) (2009) 3575-3584.
[52] W. Sulaiman, D.H. Nguyen, Transforming growth factor beta 1, a cytokine with regenerative functions, Neural Regen Res 11(10) (2016) 1549-1552.
[53] E. Nusayr, T. Doetschman, Cardiac development and physiology are modulated by FGF2 in an isoform-and sex-specific manner, Physiological Reports 1(4) (2013).
[54] M.C. den Haan, R.W. Grauss, A.M. Smits, E.M. Winter, J. van Tuyn, D.A. Pijnappels, et al. Cardiomyogenic differentiation-independent improvement of cardiac function by human cardiomyocyte progenitor cell injection in ischaemic mouse hearts, J Cell Mol Med 16(7) (2012) 1508-1521.
[55] Y. Oh, G.S. Cho, Z. Li, I. Hong, R.J. Zhu, M.J. Kim, Y.J. Kim, E. Tampakakis, et al. Functional Coupling with Cardiac Muscle Promotes Maturation of hPSC-Derived Sympathetic Neurons, Cell Stem Cell 19(1) (2016) 95-106.

SUPPLEMENTAL FIGURES

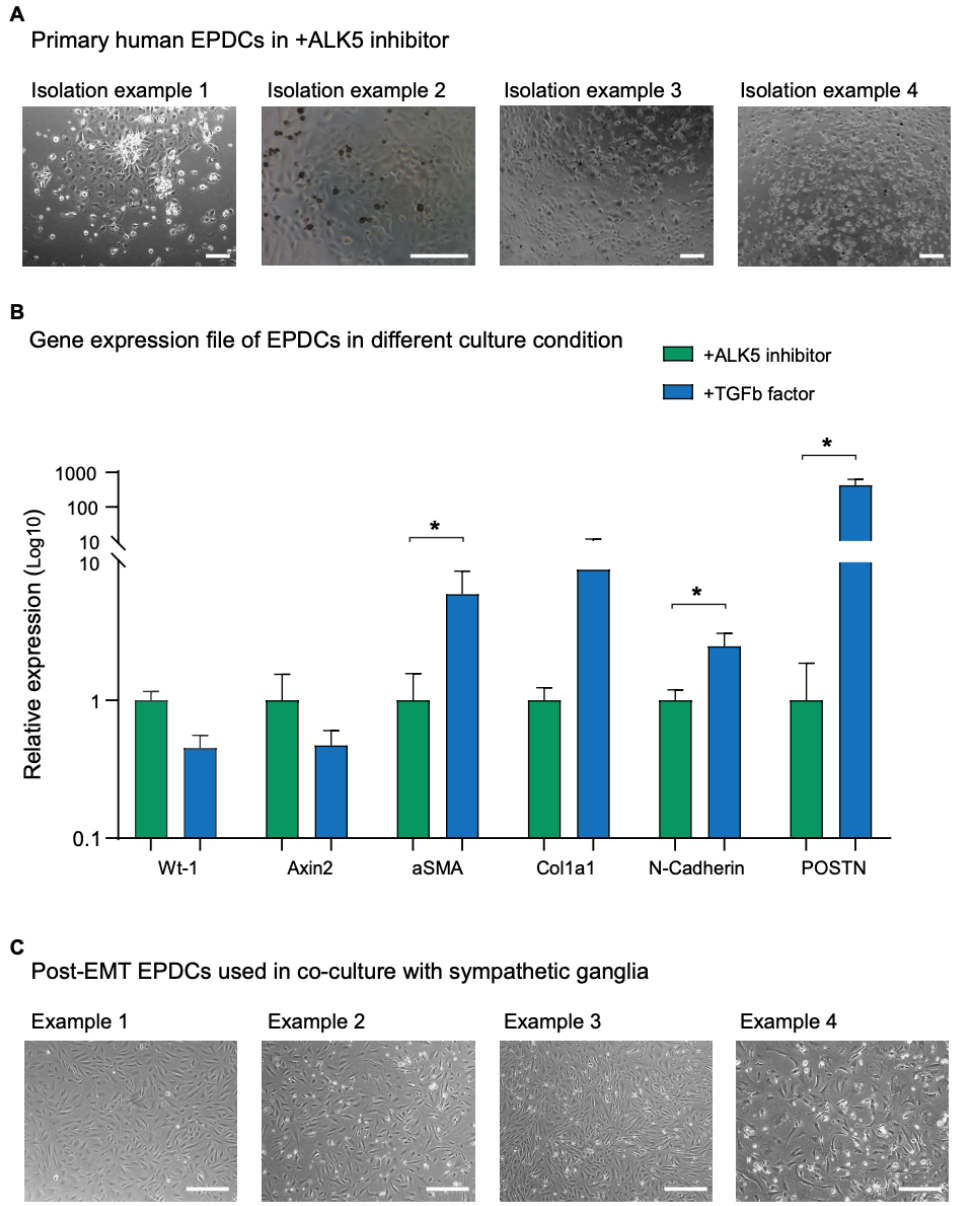

Figure S1. Supplemental information of EPDCs used in the experiment. A. Representative example bright view images of primary human EPDCs with cobblestone morphology in a culture condition supplemented with ALK5 inhibitor. Scale bar=200μm. B. Gene expression profile of cobblestone EPDCs (+ALK5 inbitor) and EPDCs undergoing EMT (+TGFb). The graph is shown as mean±SD, a paired T-test was

applied (n=2). C. Representative example bright view images of human post-EMT mesenchymal EPDCs with spindle-like morphology. Scale bar=200µm.

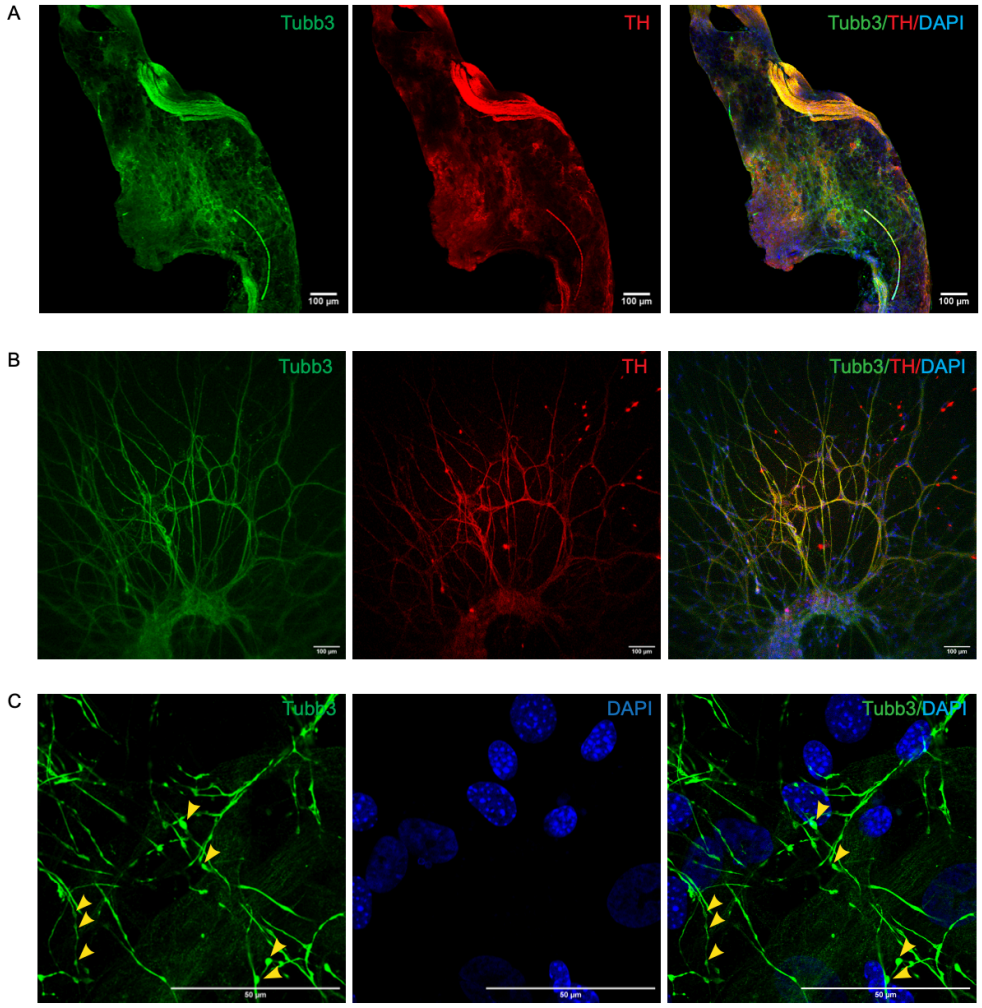

Figure S2. Sympathetic phenotype and varicosities in cultured cervical ganglia. A. Freshly isolated mouse superior cervical ganglia (SCG) that fixed immediately after isolation, whole-mount immunofluorescent staining was applied. Scale bar=100µm. B. Mouse SCG that co-cultured with myocardium and EPDCs in vitro for 6days, whole-mount immunofluorescent staining was performed after fixation. Scale bar=100µm. C. Mouse SCG that co-cultured with EPDCs in a monolayer to visualize sympathetic varicosities (indicated with arrowheads). Scale bar=50µm.

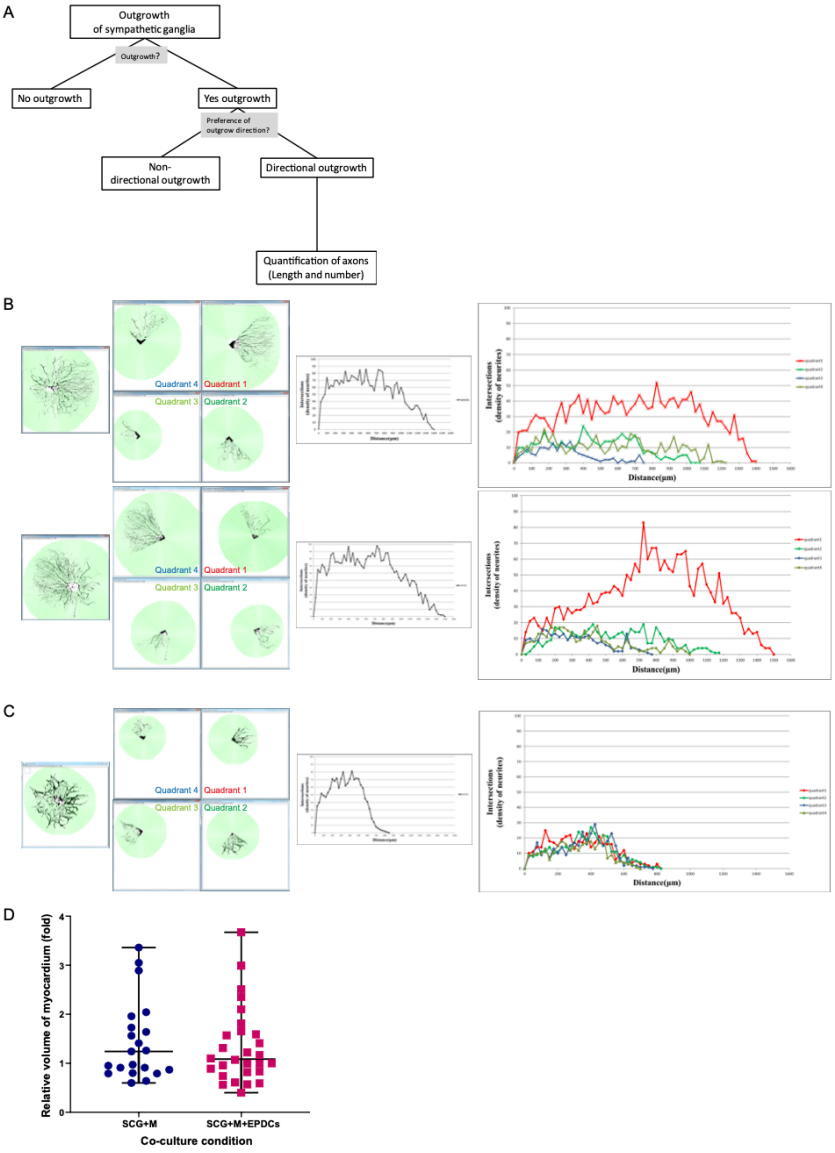

Figure S3. Quantification of neurites density in quadrants. A. Flow diagram of the work procedure. B. Neurite numbers in each quadrants-split image were quantified with NeuriteJ. The results of each quadrant were depicted in a graph. Outgrowth was designated as "directional" when outgrowth of denser and longer neurites sprouting towards the myocardium/EPDCs was observed in quadrant 1 (depicted here as the red lines in the graph on the right side of panel B). C. When each quadrant showed a similar neurite density and length, as was the case when SCG were co-cultured with EPDCs only, the outgrowth was designated "non-directional". In this case, lines depicting the different quadrants (indicated by different colors) overlap in the graph shown on the right side of panel C. D. Relative volume

of myocardium used in each co-culture is shown as medium±range. SCG+M: superior cervical ganglia with only myocardium; SCG+M+EPDCs: SCG co-culture with myocardium and EPDCs.

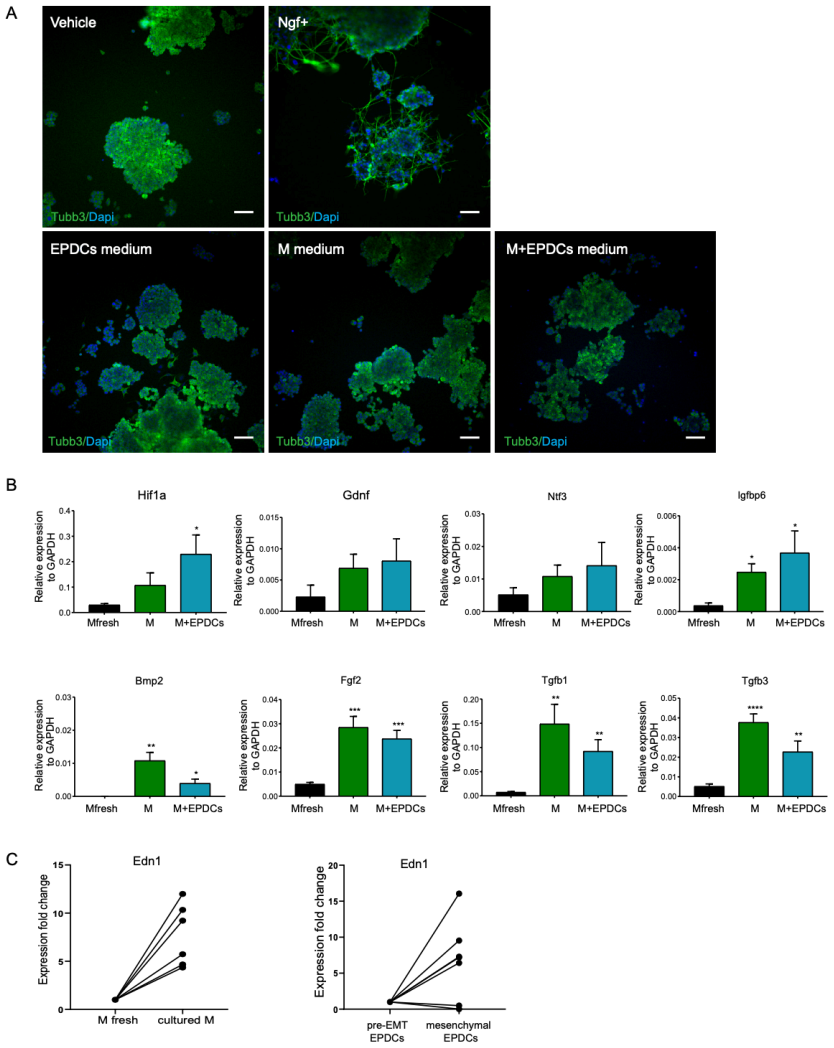

Figure S4. Related to figure 3 and figure 4. EPDCs increase neurite outgrowth by NGF in paracrine fashion. A. Tubb3 staining of PC12 cells cultured in conditioned medium as is indicated in the graph without the pre-treatment of NGF. Scale bar =100µm. B. Gene expression in fresh isolated myocardium, cultured myocardium and the myocardium co-cultured with EPDCs (n=6). Mfresh = freshly isolated myocardium; M = cultured myocardium; M+EPDCs = myocardium co-cultured with EPDCs. * $p<0.05$, ** $p<0.01$ compare to Mfresh. C. Expression of endothelin 1 (EDN1) as examined with real time PCR in cultured myocardium (cultured M) compared to freshly isolated myocardium(Mfresh) and in mesenchymal EPDCs compared to pre-EMT EPDCs. $P<0.05$ in both.

SUPPLEMENTAL METHODS

Experimental animals

C57BL/6J (the Jackson Laboratory) adult mice (n=42) and embryos of embryonic day (E) 18.5 (n=81) were used. All animal experiments were carried out according to the Guide for the Care and Use of Laboratory Animals published by NIH and approved by the Animal Ethics Committee of the Leiden University (Leiden, The Netherlands, license number AVD1160020185325).

MI induction

MI was induced in 8-week C57BL/6J mice (n=4) by permanent ligation of left anterior descending artery. Mice were anesthetized with isoflurane 5% for induction and 1.5-2% for maintenance. Mice were placed in a supine position on a controlled heating pad, intubated and ventilated mechanically (Harvard Ventilator) with a tidal volume of 240 µL and a frequency of 200/min. The thoracic cavity was opened in the fifth intercostal space. After opening of the pericardial sac, the left anterior descending coronary artery (LAD) was visualized and permanently ligated using 7.0 suture (Prolene, Johnson and Johnson, New Brunswick, NJ, USA) [1].

Human cardiac tissue collection for EPDCs

EPDC were derived from human auricle specimens, obtained as redundant material during cardiac surgery. Patients gave informed consent for use of these tissues for research purposes. All experiments were performed according to the guidelines of the Leiden University Medical Centre (Leiden, The Netherlands) and approved by the local Medical Ethics Committee.

Isolation and culture of human EPDCs

EPDCs were isolated from adult human cardiac tissue as previously described [2]. Briefly, epicardium was dissected from underlying myocardium and processed into small pieces followed by 0.25% Trypsin /EDTA (1:1; Serva and USH products) digestion for 30 min at 37°C. After digestion, the cell suspension was passed through a 100-µm cell strainer (BD Falcon), resuspended and plated on 0.1% gelatine-coated dishes. The freshly isolated EPDCs were first cultured in the complete medium supplemented with ALK5-kinase inhibitor SB431542 (5–10 µm; Tocris Bioscience, Ellisville, MO, USA) to keep EPDCs at epithelial state. EPDCs were passaged twice with 0.05% Trypsin-EDTA (Invitrogen) when reaching confluency. Complete medium is a mixed medium of Dulbecco's modified Eagle's medium (DMEM-low glucose; Invitrogen) and Medium 199 (M199; Invitrogen) in 1:1 with 10% heat-inactivated fetal calf

serum (FCS; Gibco), and 1% penicillin/streptomycin (Gibco). To obtain EPDCs of mesenchymal state, EPDCs were induced to undergo EMT by further culturing in complete medium supplemented with 1 ng/ml transforming growth factor beta 3 (TGFβ3) for 5 days. All EPDCs used in the described experiments were of between 6 to 9 passages. RNA was isolated from EPDCs after 5-day culture in ALK5-kinase inhibitor or in TGFβ3. Gene expression of epithelial EPDCs marker and mesenchymal markers were examined by real time PCR.

Preparation of human EPDCs aggregates

Human mesenchymal EPDCs around passage 6 to 9 were collected and split into sterilized microtubes at a density of 10^4 cells per tube. After centrifugation at 1,000 rpm for 4 min, the supernatant was removed and 4 µl collagen gel mix was added to each cell pellet attached to the tube bottom without mixing. Microtubes were incubated for 10 min in a cell incubator after which 80 µl complete medium was carefully added. The aggregates were then cultured for 4 days.

Dissection and culture of adult murine myocardium

Pregnant mice were sacrificed in a CO2 chamber. Uteri containing the E18.5 embryos were removed and transferred to cold PBS for short time storage on ice. The heart of the mother mouse was dissected and transferred into cold PBS as well. Atria, epicardium and endocardium were first removed from the ventricles. Subsequently, left ventricular myocardium was processed into small pieces of similar size of 0.1 mm3 under a stereo microscope. All myocardial explants were first allowed to attach to the bottom of 24-well plate by incubating at 37°C for 20 minutes, supplying a drop of complete medium to avoid tissue dehydration. All myocardial explants were then cultured in 500 ul/well complete medium in a cell incubator (at 37°C and 5% CO2) for 7 days to induce myocardial damage and subsequently used for co-culture assays.

Dissection of embryonic sympathetic ganglia

After resection of the uteri with the E18.5 embryos, the embryos were collected and euthanized in cold PBS. To isolate superior cervical ganglia (SCG), the embryonic skin was opened along the midline of the neck using a sharp forceps, exposing the bilateral bifurcations of the common carotid arteries. This was used as reference to indicate the location of cervical ganglia by removing ventral cervical muscle tissue. Cervical ganglia were first dissected together with carotid arteries and placed in cold PBS. Thereafter, vascular and connective tissues were removed. Each isolated SCG was subsequently processed into 3-4 tiny pieces under a stereo microscope for subsequent culturing.

Sympathetic ganglion culture and neurite outgrowth assay

General ganglion culture methods. To provide a 3-dimensional environment for neurite projections from ganglia, we used a similar gel culture method of ganglia as reported in 1997 [3]. In the current study, type I collagen gel mix (Corning 35429) 1,5 ml, 10X PBS 500 µl, 1N NaOH 34.5 µl and complete medium 3 ml were mixed under sterile conditions and handled on ice. For ganglion explant cultures, 20 µl collagen gel mix was placed at the bottom of 24-well plates. Once collagen gel got solidified (10 min in a cell incubator), cervical ganglion pieces with or without other co-culture cells/tissue were transferred onto the solidified gel drops and another 50 µl collagen gel mix was added to encapsulate the ganglion explants. The plate was kept in the incubator for 20 min before 500 µl complete culture medium was added. For purpose of high magnification imaging of neurites, cervical ganglion pieces were co-cultured with EPDCs as a monolayer in a 48-well plate with coverslips. Briefly, ganglia pieces were first allowed to attach to the surface of coverslips in 48-wel plate by incubating at 37°C for 20 minutes, supplying a drop of complete medium to avoid tissue dehydration. Then 200 ul complete medium containing 2x10^4 EPDCs were added.

Neurite outgrowth assay. To detect the function of EPDCs on neurite outgrowth and extension, ganglion explants from embryos were randomly cultured in 5 conditions:

Vehicle: 1-2 ganglia explants cultured in gel; +EPDCs: 2 ganglion explants co-cultured with 1 EPDCs aggregate ; +M+EPDCs: 2 ganglion explants with 1 EPDCs aggregate and 1 cultured myocardial (M) piece; +M: 2 ganglion explants with 1 piece of cultured adult myocardium; and +M-fresh: 2 ganglion explants co-cultured with 1 freshly dissected piece of adult myocardium (M fresh) .

Immunostaining of ganglion explants

After 6-day culture, the medium in the culture plates was removed followed by rinsing with PBS and fixation with 4% PFA for 30 min (10 min for ganglia co-cultured with EPDCs in a monolayer). To make the explants better accessible for antibodies the gels were treated with 0.5% Tween 20 for 30 min (10 min for monolayer) after which blocking with 1% BSA in PBS with 0.05% Tween 20 was carried out for 1 hr. The cultures were stained with primary antibody rabbit anti β-Tubulin III (anti-Tubb3) (Sigma T2200; 1:500) (a general staining for autonomic nerve fibers), Tyrosine hydroxylase (anti-TH) (ThermoFisher PA14679; 1:500) overnight at 4°C. After 3 times rinsing with PBS, visualization of the primary antibodies was done with Alexa Fluor-488 donkey anti-rabbit IgG(H+L) (Life Technology A-21206; 1:250), Alexa Fluor-568 donkey anti-sheep IgG(H+L) (Life Technology A21099; 1:250). After 2,5 hr incubation (1 hr for monolayer) with the secondary antibodies at room temperature, the explants were rinsed

again with PBS. DAPI was used to stain nuclei. Images of ganglia were captured with Leica AF6000 microscope and Leica SP8 confocal microscope.

Whole-mount immunofluorescent staining and clearing of freshly isolated sympathetic ganglion

Freshly isolated cervical ganglia were fixed with 4% PFA at 4°C overnight followed by a treatment with 0.5% Tween 20 for 40 min. After the blocking in 1% BSA in PBS with 0.05% Tween 20 for 1 hr, the ganglia were incubated with primary antibody: rabbit anti β-Tubulin III (anti-Tubb3) (Sigma T2200; 1:500) (a general staining for autonomic nerve fibers) and Tyrosine hydroxylase (anti-TH) (ThermoFisher PA14679; 1:500) for 24 hr at 4°C. After 3 times rinsing with PBS, visualization of the primary antibodies was done with Alexa Fluor-488 donkey anti-rabbit IgG(H+L) (Life Technology A-21206; 1:250) and Alexa Fluor-568 donkey anti-sheep IgG(H+L) (Life Technology A21099; 1:250) at 4°C overnight. DAPI was used to stain nuclei. Images were immediately captured with Leica SP8 confocal microscope after tissue clearing with BABB solution[4]. Briefly, the ganglia were dehydrated in 70% and 100% methanol for 5min after staining. Methanol was first replaced first with 50% (vol/vol) BABB/ methanol then 100% BABB, let ganglia stay in 100%BABB for a few minute until clear.

Quantification of neurite outgrowth

A method to quantify “directional” (i.e towards myocardium) outgrowth of neurites was developed based on different existing plugins (Quadrant Picking and NeuriteJ) in ImageJ. To measure the length of neurites, as well as the density of neurites in each culture condition, ImageJ 1.51s software (National Institutes of Health, Bethesda, MD) was used to process and analyze all β-Tubulin III+ (Tubb3+) images. First, all outgrowth results were classified into 3 groups (no outgrowth, non-directional outgrowth and directional outgrowth) according to the presence of neurite outgrowth and its directional preference as is illustrated in Fig. S3A. Once directional outgrowth was detected, anti-Tubb3 images were processed by the Quadrant picking plug-in, which divided the image in 4 quadrants according to the ganglion-myocardium position. The quadrants were numbered 1 to 4, where Quadrant 1 was the one facing the myocardium/EPDC aggregate, followed clockwise by quadrant 2 to 4 (Fig. 2B). Thereafter, the neurites sprouting towards myocardium/EPDCs were quantified with NeuriteJ as described by Torres-Espin at al. [5]. Briefly, SCG explants were identified and circles (with an interval of 25 μm) surrounding SCG were produced automatically in NeuriteJ (as is shown in the left panel of Fig. S3B, C). The number of directional neurites was automatically calculated by counting cross point of neurites and circles.

To correct for potential differences in amount of myocardium used in each experiment, all data were normalized for myocardial volume. The myocardial volume was calculated based on confocal images. The normalized directional neurite outgrowth was calculated as: Normalized directional neurite number = Counted neurite number/Relative myocardium volume. The volume of each myocardium used in each co-culture were measured with a confocal microscope (Leica SP8) by detecting autofluorescence of myocardium. Z-stack (10 um per step) and tile scan options of confocal microscopy were applied during imaging. Volume of myocardium = stacked area of all stacks * thickness per step (10 um). The myocardium volume of the myocardium used in the first co-culture was considered as reference volume, and the relative myocardium volume of the rest of the myocardium was calculated. Normalized directional neurite number = Counted neurite number/Relative myocardium volume.

Collection of conditioned medium

To collect condition medium, isolated left ventricular myocardium tissues (after removal of epicardium and endocardium) were either co-cultured with mesenchymal EPDCs or cultured exclusively in complete medium (as is described above) for 4 days. Next, the tissues and cells were cultured with serum-free DMEM/F12 medium for 48 hr for the purpose of collecting serum-free conditioned medium. The collection of conditioned medium was repeated 3 times with a 1-day culturing interval with complete medium between each collection.

The collected serum-free medium included: EPDCs medium (derived from culturing only EPDCs); EPDCs+M medium (of co-cultured myocardium and EPDCs) and M medium (of cultured myocardium only).

PC12 neurite outgrowth assay

PC12 cells were cultured in proliferation medium (DMEM medium supplemented with 10% HS (Horse serum, Gibco), 5% FCS(Gibco) and 1% penicillin/streptomycin (Gibco)) prior to the neurite outgrowth assay for expansion. To examine the differentiation of PC12, PC12 cells were seeded on a 48 well-plate pre-coated with 50 ng/ml type I collagen at a density of 2,000 cells per well in proliferation medium overnight and then cultured in vehicle medium (DMEM/F12 medium, 1% FCS, 1% penicillin/streptomycin), NGF differentiation medium (supplemented with 50 ng/ml NGF), or the medium mixed with 1/3 volume of DMEM/F12 medium and 2/3 volume of conditioned medium, 1% FCS, 1% penicillin/streptomycin. Replicates of each culture condition were applied. The media were refreshed once on the second day and the PC12 cells in each medium were fixed with 4% PFA on the fourth day. The PC12 cells were permeabilized with 0.5% Tween-PBS for 10 min and blocked in 1% BSA/0.05% Tween-PBS for 1 hr at room temperature. The cells were afterwards incubated with rabbit

anti-β-Tubulin III (Sigma T2200; 1:500) overnight at 4°C and with Alexa Fluor-488 donkey anti-rabbit IgG(H+L) (Life Technology A-21206;1/200) for 1 hr at room temperature. DAPI was used to visualize nuclei. Fluorescence images of entire wells were captured with an EVOS cell imaging system and used for neurite differentiation quantification of PC12 cells. To calculate the ratio of neurite numbers/total cell numbers of each culture condition, 6 fields in each well were used for counting neurites and cells, using ImageJ software. Representative images were captured with an Leica AF6000 fluorescent imaging system.

Supplemental table 1. Experimental setup of PC12 cells cultured in conditioned medium without pre-treatment with NGF.

Condition	Day 0 - 6
Vehicle	- NGF
NGF50+	+ NGF
EPDCs med	EPDCs med
M med	M med
M+EPDCs med	M+EPDCs med

Supplemental table 2. Experimental setup of PC12 cells cultured in conditioned medium with 2-day pre-treatment with NGF.

Condition	Day 0 - 2	Day 3 - 6
Vehicle	- NGF	- NGF
Ngf50+/-	+ NGF (trigger)	- NGF
Ngf50+/+	+ NGF (trigger)	+ NGF
EPDCs med	+ NGF (trigger)	- NGF + EPDCs med
M med	+ NGF (trigger)	- NGF + M med
M+EPDCs med	+ NGF (trigger)	- NGF + M+EPDCs med

Real time PCR (RT-PCR)

To study the impact of mesenchymal EPDCs on the expression of nerve growth related genes in myocardium, left-ventricular myocardium explants (fresh isolated or cultured for 7 days in vitro) were cultured exclusively or co-cultured with EPDC aggregates for 2 days. Afterwards, myocardial explants were collected for gene expression analysis. Briefly, RNA was extracted with NucleoSpin RNA (Macherey-Magel). After treatment with DNase (DNA-free kit, Invitrogen) and cDNA synthesis (iScript DNA synthesis kit, Bio-Rad), RT-PCR was performed by using SYBR Green (Bio-Rad) and run on Real-time system (Bio-Rad) for 44 cycles and checked by electrophoresis on a 2% agarose gel. Primers used for RT-PCR are shown in Supplement table3.

Supplemental table 3. Primer sequences

Gene		Sequence
Gapdh	Forward	TTGATGGCAACAATCTCCAC
	Reverse	CGTCCCGTAGACAAAATGGT
Ngf	Forward	ATGGTGGAGTTTTGGCCTGT
	Reverse	GTACGCCGATCAAAAACGCA
SEMA3A	Forward	AGAAATGACCGTCTTCCGGG
	Reverse	TGCACAGGCTTTGCCATAGA
Edn1	Forward	GGCCCAAAGTACCATGCAGA
	Reverse	TGCTATTGCTGATGGCCTCC
Gdnf	Forward	TATCACTCCCTTTGTGGCTGC
	Reverse	GGGTGTGGAACCATGCGAA
Ntf3	Forward	GGAGTTTGCCGGAAGACTCTC
	Reverse	GGGTGCTCTGGTAATTTTCCTTA
Hif1α	Forward	TTGCTGAAGACACAGAGGCA
	Reverse	TCATCAGTGGTGGCAGTTGTG
FGF2	Forward	GCCAACCGGTACCTTGCTAT
	Reverse	GTCCCGTTTTGGATCCGAGT
Tgb1	Forward	GTCACTGGAGTTGTACGGCA
	Reverse	GTTTGGGGCTGATCCCGTT
Igfbp6	Forward	TGCTAATGCTGTTGTTCGCTG
	Reverse	CACGGTTGTCCCTCTCTCCT
Bmp2	Forward	TGCTAGATCTGTACCGCAGG
	Reverse	GGCCGTTTTCCCACTCATCT
Tgfb1	Forward	GTCACTGGAGTTGTACGGCA
	Reverse	GTTTGGGGCTGATCCCGTT
Tgfb3	Forward	TGTCACACCTTTCAGCCCAA
	Reverse	GGGTTGTGGTGATCCTTTTGC
EdnrA	Forward	TACAAGGGCGAGCTGCATAG
	Reverse	CCGTTCCTCCTGTTGAGCAT

WES (automated Western Blots) procedure

WES system (ProteinSimple) and 2-40 KDa Seperation Modules (ProteinSimple, SM-W012) were applied to detect NGF protein in fresh myocardium and cultured myocardium samples. Total protein was extracted from myocardium samples with RIPA buffer (Thermo Fischer Scientific). Total protein was measured with BCA assay and diluted with 0.1x sample buffer into the desired concentration (around 0.5 μg/μl). All procedures were performed by following the manufacturer's instruction. In brief, 4 volumes of protein sample were mixed with 1 volume of 5X Fluorescent Master Mix and heated at 95°C for 5 min. First antibody, rabbit anti-NGF (Sigma, N6655) and rabbit anti-GAPDH (abcam, ab9485) were separately prepared 1:10 in antibody diluent. The samples, antibody diluent (ProteinSimple, DM-001), primary antibodies (in antibody diluent), HRP-conjugated secondary antibodies (ProteinSimple, DM-001) and chemiluminescent substrate (ProteinSimple, DM-001) were dispensed into the specific wells of the separation module with the volumes recommended in the instruction. When the separation module and capillary cartridge were loaded in the WES system, default settings of the instruments were applied to the run under the control of Compass software. The chemiluminescent peaks were identified automatically and were checked in electropherograms in Compass. The results of area under the peak (AUP) were exported, and NGF/GAPDH ratio of AUP of each sample was afterwards calculated.

Dot blotting

SEMA3A protein expression in myocardium was examined and quantified by dot blotting. 5ug of total protein extracted from myocardium samples were loaded on the PVDF membrane within bio-dot apparent (bio-rad) and incubated for 1 min. The protein samples were subsequently filtered on the membrane by vacuum. The membrane was washed twice and incubated in blocking buffer for 1hr at RT. Next the membrane was incubated with rabbit anti-SEMA3A antibody (Abcam ab199475; 1:1000) and mouse anti-actin antibody (Millipor BV MAB1501; 1:2000) overnight at 4°C followed by an incubation with HRP-linked antibody (cell signalling #7074; 1:10,000) and anti-mouse IgG HRP-linked antibody (cell signalling #7076; 1:10,000) for 1hr at RT. SEMA3A protein was finally visualized with a WesternBright kit (Isogen life science) and images were captured by C500 western blot imaging system (Azure biosystems). The results were quantified by ImageJ.

TUNEL assay and immuno-staining of cultured myocardium explants

Left-ventricular myocardium was isolated from adult mice and processed into small pieces with the same methods of preparing myocardium explants for co-culture with ganglia. Part of the myocardium explants were fixed with 4% PFA immediately after isolation. The rest of the

myocardium explants were mono-cultured or co-cultured with mesenchymal EPDCs in complete medium for 7 days in vitro, and then fixed with 4% PFA. After embedding with paraffin, 5 µm-thick myocardium sections were made and deparaffined in xylene and ethanol. To detect apoptosis and necrosis in myocardium explants, sections of fresh and cultured myocardium explants were stained with TUNEL (TUNEL in situ cell death detection kit; Sigma Aldrich) for 90 min at 37°C. To detect NGF protein, deparaffined sections were first heated in Tris/EDTA buffer (10mM Tris PH=9.0, 1mM EDTA, 0.05% Tween) at 98°C for 15 min to unmask antigen. The sections were afterwards blocked in blocking buffer (1% BSA, 0.05% Tween in PBS) for 30min at room temperature and incubated with first antibody, rabbit-anti-beta NGF antibody (abcam ab6199; 1:100) and mouse-anti-Tropomyosin (Sigma T9283; 1:200) at 4°C overnight. The sections were rinsed 3 times in PBS and 0.05% Tween-PBS and incubated with fluorescence-labelled secondary antibody, Alexa Fluor 488 goat-anti-rabbit IgG(H+L) (Life technology A-11034; 1:200) and Alexa Fluor 568 goat-anti-mouse IgG1 (Life technology A-21124; 1:200) at room temperature for 1 hr. Nuclei were stained with DAPI and the sections were mounted with Prolong Gold antifade reagent (Life technology P36965). Images were captured with Leica SP8 confocal microscope. To evaluate the NGF expression in myocardium explants and post-MI hearts, 3 sections of each myocardium explants and 3 sections of each post-MI hearts were chosen for quantification. NGF expression in 3 areas of each sections was quantified in ImageJ, averaged and calculated as the percentage NGF area out of the total tissue area.

Sirius red and Immuno-staining of post-MI hearts

7 days after MI surgery, mice were euthanized and the hearts were isolated. The MI hearts were fixed in 4% PFA and paraffin embedded. 5µm-thick heart sections were first de-paraffined with xylene and ethanol and then processed with Sirius red staining and immunofluorescence staining with first antibodies: rabbit anti-beta NGF (Abcam ab6199; 1:100), mouse anti-Tropomyosin (Sigma T9283; 1:200), rabbit anti-Wilms tumor 1 (anti-WT-1) (Abcam ab89901; 1:100).

To perform Sirius red staining, deparaffined sections were first stained with Weigert's iron haematoxylin for 10min followed by Pirco-Sirius red (0.1% Sirius red in saturated picric acid) staining for 60min. The sections were washed twice in acidified water (2.5 ml acetic acid in 500 ml distilled H2O), dehydrated and mounted with Entellan.

To perform immunofluorescence staining, deparaffined the sections were first treated with Tris/EDTA buffer (10mM Tris PH=9.0, 1mM EDTA, 0.05% Tween) at 98°C for 15 min. After cooling down at room temperature, the sections were rinsed in PBS and 0.05% Tween-PBS, then the section were incubated with first antibodies (diluted in 1% BSA, 0.05% Tween-PBS

into desired concentration as is described above) at 4°C overnight. On the next day, the sections were rinsed with PBS and 0.05% Tween-PBS followed by the incubation of fluorescence labelled secondary antibodies according to the species of first antibody at room temperature for 1 hr. Secondary antibodies used included: Alexa Fluor 488 donkey-anti-rabbit IgG(H+L) (Life technology A-21206; 1:200), Alexa Fluor 594 goat-anti-mouse IgG(H+L) (Life technology A-21203; 1:200). Nuclei were stained with DAPI and the sections were mounted with Prolong Gold antifade reagent (Life technology P36965). Images were captured with Leica SP8 confocal microscope.

Statistics

Graphs are presented as mean ± SEM. The presence of neurite outgrowth in control and EPDCs co-culture groups were compared using a Chi-square test. The Chi-square test was also used to compare the proportion of neurite outgrowth between the different co-culture groups (ganglion/myocardium, ganglion/myocardium/EPDC co-cultures). Neurites density at different lengths in the Myocardium condition and Myocardium-EPDCs condition were compared using an independent Student's t test (two-sided). PC12 neurite outgrowth in different conditioned media were compared using one-way ANOVA. Gene and protein expression in myocardium were compared using one-way ANOVA. Results were considered significant when the p value was <0.05. GraphPad Prism (GraphPad Software, San Diego, CA, USA; version 6) was used for statistical analysis.

REFERENCE

[1] E.M. Winter, R.W. Grauss, B. Hogers, J. van Tuyn, R. van der Geest, H. Lie-Venema, R.V. Steijn, S. Maas, M.C. DeRuiter, A.A.F. de Vries, P. Steendijk, P.A. Doevendans, A. van der Laarse, R.E. Poelmann, M.J. Schalij, D.E. Atsma, A.C. Gittenberger-de Groot, Preservation of left ventricular function and attenuation of remodeling after transplantation of human epicardium-derived cells into the infarcted mouse heart, Circulation 116(8) (2007) 917-927.

[2] E. Dronkers, A.T. Moerkamp, T. van Herwaarden, M.J. Goumans, A.M. Smits, The Isolation and Culture of Primary Epicardial Cells Derived from Human Adult and Fetal Heart Specimens, Jove-J Vis Exp (134) (2018).

[3] S.E. Blackshaw, S. Arkison, C. Cameron, J.A. Davies, Promotion of regeneration and axon growth following injury in an invertebrate nervous system by the use of three-dimensional collagen gels (vol 264, pg 657, 1997), P Roy Soc B-Biol Sci 264(1384) (1997) 1101-1102.

[4] T. Yokomizo, T. Yamada-Inagawa, A.D. Yzaguirre, M.J. Chen, N.A. Speck, E. Dzierzak, Whole-mount three-dimensional imaging of internally localized immunostained cells within mouse embryos, Nat Protoc 7(3) (2012) 421-431.

[5] A. Torres-Espin, D. Santos, F. Gonzalez-Perez, J. del Valle, X. Navarro, Neurite-J: An Image-J plug-in for axonal growth analysis in organotypic cultures, J Neurosci Meth 236 (2014) 26-39.